Title
THE SPECTROSCOPY OF 54Fe VIA THE REACTION 54Fe(p,p'y) 54Fe AT 10 MeV

Authors
Moss, J.M.
Hendrie, D.L.
Glashausser, C
et al.

Publication Date
1972-04-01

Published in Nuclear Physics A
194, pp. 12-48, 1972

LBL-1683

THE SPECTROSCOPY OF ^{54}Fe VIA THE REACTION $^{54}Fe(p, p'\gamma)^{54}Fe$ AT 10 MeV

J. M. Moss, D. L. Hendrie,
C. Glashausser, and J. Thirion

April 1972

Prepared for the U. S. Atomic Energy Commission
under Contract W-7405-ENG-48

DISCLAIMER

1.E.4:2.B *Nuclear Physics* A194 (1972) 12—48; © *North-Holland Publishing Co., Amsterdam*

THE SPECTROSCOPY OF ^{54}Fe VIA THE REACTION ^{54}Fe(p, p'γ)^{54}Fe AT 10 MeV

J. M. MOSS †, D. L. HENDRIE, C. GLASHAUSSER †† and J. THIRION †††
Lawrence Radiation Laboratory, Berkeley, California 94720

Received 21 April 1972

Abstract: In the ^{54}Fe(p, p'γ)^{54}Fe reaction at 10 MeV, angular correlations of gamma rays coincident with protons detected near 180°, have been measured. From an analysis of the angular correlations, unambiguous spin assignments have been made for the 3.345(3), 4.074(3), 4.579(2), 4.781(3), and 4.949(4) MeV states. Model-dependent spin assignments have been made for several other states. The angular correlation analysis also yielded multipole mixing ratios for many transitions and branching ratios for the decay of all states of ^{54}Fe below 5 MeV. From the same data, an analysis of the Doppler shifts of the coincident gamma rays allowed determination of the lifetimes of the 1.409, 2.959, 3.164, 3.836, 4.048, 4.074, 4.265, 4.287, 4.781 and 4.949 MeV states. Utilizing all the measured quantities, estimates have been of the strengths of 20 E2, 9 M1, and 4 E1 transitions. To aid in understanding the nature of the observed levels, the positions of various *np-mh* states have been estimated using a monopole residual interaction. It is found that 2p-4h states as well as 1p-3h states may occur at low excitation energies. The 2.540 MeV (0_2^+) state is probably of the configuration 2p-4h. The decay properties of all states below 3.5 MeV are compared to the predictions of theoretical calculations in which 1p-3h proton ($2p_{\frac{1}{2}}$ and $1f_{\frac{1}{2}}$) excitations were considered.

E NUCLEAR REACTIONS ^{54}Fe(p, p'), $E_p = 10$ MeV; measured $\sigma(E_{p'}, E_\gamma, \theta_{p'\gamma})$, Doppler-shift attenuation. ^{54}Fe deduced levels, γ-mixing, J, $T_{\frac{1}{2}}$, γ-branching.

1. Introduction

1.1. GENERAL

In the simple shell-model picture, if ^{56}Ni is considered to have a doubly closed shell, the ground state of ^{54}Fe consists of two $1f_{\frac{1}{2}}$ proton holes coupled to zero. The low-energy spectrum of ^{54}Fe should then have three states of the configuration $(f_{\frac{1}{2}})_J^{-2}$, where $J = 2, 4, 6$. A similar situation occurs in ^{50}Ti which has the proton configuration $(f_{\frac{1}{2}})_J^2$ outside the ^{48}Ca core. The low-energy spectra of these two nuclei show striking differences. ^{50}Ti exhibits the expected 2^+, 4^+, 6^+ sequence and has no additional states below 4.16 MeV. In contrast ^{54}Fe, while having three states identifiable as $f_{\frac{1}{2}}^{-2}$, also has several other states in the same energy region. The problem of low-lying states not accounted for by $f_{\frac{1}{2}}^n$ configurations is, of course, not unique

† Present address: School of Physics and Astronomy, University of Minnesota, Minneapolis, Minnesota 55455.
†† Present address: Rutgers University, New Brunswick, New Jersey.
††† Permanent address: CEN-Saclay, 91 Gif-sur Yvette, France.

to ^{54}Fe [ref. [1])]. A case intermediate between ^{54}Fe and ^{50}Ti is found in ^{42}Ca where 4p-2h and 6p-4h states intrude in a $f_{\frac{7}{2}}^2$ neutron spectrum.

Only recently has much theoretical effort been devoted to understanding the states of ^{54}Fe. The large configuration space required to make reasonable calculations has undoubtedly been an inhibiting factor. Additionally, until recently, very little experimental information would have been available for comparison to theory.

Experimentally ^{54}Fe is a rather difficult nucleus to investigate. It is not accessible to single nucleon transfer reactions. Furthermore, inelastic scattering experiments[2-6]) have been hampered by the fact that many of the levels are quite closely spaced and hence are unresolvable. Indeed, even the reliable assignment of spins to the levels of ^{54}Fe has been rather difficult; in the (p, p'γ) angular correlation work of Thomas *et al.* [7]), several low-lying levels of ^{54}Fe could not be resolved and therefore could not be assigned spins. The purpose of this work then was the further elucidation of the character of the excited states in ^{54}Fe, with the hope that some insight might be gained into the larger problem of nuclear structure in the region of the ^{56}Ni doubly closed shell. To this objective we have used the (p, p'γ) angular correlation method in the investigation; this technique was extended in the present work by the use of a large-volume, high-resolution Ge(Li) gamma detector. The information obtained from an analysis of the angular correlations included several new spin assignments, multipole-mixing ratios for many electromagnetic transitions, and branching ratios for the decay of all states below 5 MeV. In addition, it was possible to extract from the same data several excited state lifetimes using a Doppler-shift attenuation analysis.

1.2. ANGULAR CORRELATION METHOD

For the study of the levels of ^{54}Fe we have used the technique, first described by Litherland and Ferguson [8]) (method II), which has, in the last five years, become a standard tool for in-beam nuclear spectroscopy. The geometry used, commonly called collinear, is that in which one measures angular distributions of γ-rays in coincidence with particles scattered at 0° or 180°. The great utility of collineary geometry resides in the fact that the substate population is quite restricted.

It can be shown [8]) that, when the outgoing particles are detected along the z-axis, the maximum possible angular momentum projection of the residual nucleus is given by: $m_{max} = S_i + S_0 + a$, where S_i and S_0 are the spins of the incoming and outgoing particles, respectively, and a is the initial nuclear spin. In the present case of the (p, p') reaction on a spin-zero nucleus, only the $m = 0, \pm 1$ substates of the residual nucleus can be populated. The axial symmetry of the system implies equal population of the $m = \pm 1$ substates ($P(1) = P(-1)$). Therefore, the unknown parameters of the angular correlation are $P(0)$, $P(1)$, and δ, where δ is the multipole mixing ratio of the γ-transition. The general angular correlation function for the reaction may be written:

$$W(\theta_\gamma) = \sum_k A_k P_k(\cos\theta_\gamma) = \sum_k \rho_k(a) F_k(ab) P_k(\cos\theta_\gamma), \qquad (1)$$

where P_k are Legendre polynomials, F_k are well-known correlation coefficients and A_k or ρ_k (spherical tensors) are the parameters determined by the experiment. The formalism is that of Poletti and Warburton [9]). For a derivation of eq. (1) and a more complete description of its use, refs. [8-10]) should be consulted. We mention here only that the measured parameters A_0, A_2, and A_4 may be directly related to the unknowns previously discussed. Thus, in favorable situations, the spins and multipole mixing ratios may be unambiguously determined from a theoretical fit to the angular correlation. The expansion in terms of Legendre polynomials is limited to even integers because of the axial symmetry of the system. Furthermore, it is usually quite difficult to observe with statistical significance terms of $k > 4$, thus the expansion is terminated at $k = 4$; in general, k may have values up to $2a$.

In previous experiments employing collinear geometry, NaI(Tl) detectors have been used to detect the de-excitation γ-rays. These detectors are characterized by high detection efficiency and rather poor energy resolution. The best resolution obtainable in such an experiment is that of the particle counter and is usually limited to $\sim$ 50 keV. Thus, the usefulness of this powerful spectroscopic technique has been restricted to levels which could be cleanly resolved in the particle spectrum.

A primary goal of this work was the extension of the spectroscopic method, previously described, by the use of a high-resolution Ge(Li) counter for detection of the γ-rays. This extension was made possible by two advances in γ-ray counting technology. These are: i) The advent of large-volume germanium detectors, and ii) the development of a high count-rate amplifier system.

1.3. LIFETIME MEASUREMENTS

An important class of methods for measuring nuclear lifetimes utilizes the Doppler shift observed when γ-decay occurs from a nucleus traveling with a velocity, v. The Doppler shift, ΔE_0, is then,

$$\Delta E_0 = E - E_0 = E_0(v_0/c)\cos\theta, \tag{2}$$

where E_0 and E are the unshifted and shifted γ-ray energies, respectively, and θ is the angle of observation of the γ-ray with respect to the velocity vector, v_0, of the recoiling nucleus. The particular technique utilized in the present experiment was the Doppler-shift attenuation method (DSAM); various modifications of the DSAM have been described by several authors [11-14]). The optimum condition for the application of the DSAM is that the average recoil velocity, v_0, be a well-defined and calculable quantity. This implies a coincidence with the detected particle from the reaction producing the recoil. Fortunately, the geometry which has been used in past experiments of this type is identical to that required for the present angular correlation experiment. With this geometry, γ-rays are detected only from nuclei which recoil in the beam direction (to a good approximation) and, thus have the maximum possible recoil energy. The velocity vector, v_0, may be calculated simply from the kinematics of the reaction.

To utilize the Doppler-shift information, the lifetime (τ) of the state must be of the order of the stopping time (τ_s) of the recoil nucleus in the target. In such a case, the maximum Doppler shift as given by eq. (2) will be attenuated by a factor $F(\tau)$, where

$$F(\tau) = (1/\tau)\int_0^\infty (v(t)/v_0)\exp(-t/\tau)\mathrm{d}t. \tag{3}$$

In order to obtain $v(t)$, we use the relation $\mathrm{d}E/\mathrm{d}x = mv\,\mathrm{d}v/\mathrm{d}x = m\,\mathrm{d}v/\mathrm{d}t$, where $\mathrm{d}E/\mathrm{d}x$ is the stopping power of the recoil ion in the stopping medium. Since there is little experimental data available on stopping powers of low-energy ($v/c < 137$) heavy ions, it is necessary to rely on theoretical estimates of $\mathrm{d}E/\mathrm{d}x$. For the present analysis, the theory of Lindhard, Scharf, and Schiøtt [15]) (LSS) was used. LSS, using the Thomas-Fermi model of the atom, consider separately the electronic and the nuclear energy loss. The former arises from collisions in which atomic electrons are excited (including ionization) and is characterized by a $\mathrm{d}E/\mathrm{d}x$ which is proportional to v. The latter, which is important at low velocities, arises from elastic collisions with the ions in the target. LSS have derived a universal curve for the nuclear stopping power. Because nuclear collisions are capable of producing large-angle scattering of the recoils, it is important to include this effect in the analysis. An expression for the mean scattering angle, $\cos\phi(t)$, has been derived by Blaugrund [12]) using the theory of LSS. Thus, given the total $\mathrm{d}E/\mathrm{d}x$ over the entire velocity range of interest, it is possible to calculate for comparison to experiment:

$$F(\tau) = (1/\tau)\int_0^\infty (v(t)/v_0)\cos\phi(t)\exp(-t/\tau)\mathrm{d}t. \tag{4}$$

2. Experimental apparatus

2.1. GENERAL

The experimental facilities for γ-ray experiments at the Berkeley cyclotron have been described in a previous paper [16]). We mention here only those details required for understanding the present experiment. A beam of 10 MeV protons from the 88″ variable-energy cyclotron was focused at the target position, to a spot about 3 mm high and 1.5 mm wide. After passing through the scattering chamber, the beam was stopped in a Faraday cup, which was split vertically along the center line. Charge from each half of the Faraday cup was separately integrated and used to monitor both the beam current and alignment. Equal currents were maintained in each half to insure a constant position of the beam spot. Periodically, the beam position on the target was checked with the aid of thin scintillating target and a closed-circuit TV system. The Faraday cup was initially aligned with the known optic axis (which passed through the target position) with the aid of a transit. Before the run, slight adjustments in the beam axis were made, using the horizontal and vertical motion of the analyzing slits and two small steering magnets located near the cyclotron. The

beam was thus required to go through the target position and to be centered in the Faraday cup.

2.2. ANNULAR DETECTOR

An annular Si(Li) detector 1.5 mm thick was used to detect the scattered protons. When placed in position 6.3 cm from the target, it covered the angular range 168° – 173° and subtended a solid angle of 0.078 sr; the detector was used only in the position in which it was centered at 180°. Particles striking the detector were limited to the sensitive region by inner and outer collimators made of 1 mm thick tantalum. The inside collimator was held in place by a tube (1 mm surface thickness) which was precisely milled to fit into a hole in the back protective plate. The inside diameter of the tube was sufficient large (5 mm) to allow free passage of the beam through the detector.

In order to improve the timing characteristics of the proton detector, and to reduce the noise due to leakage current, the detector was cooled to −35 °C by means of a copper-braid strap connected to a liquid nitrogen cold-finger. The temperature of the detector, which was monitored by a thermocouple, remained constant within ±1 °C.

Because of the large size of the detector, and the short distance between it and the target, the commonly used electrostatic or magnetic electron suppression devices were impractical. Thus, to eliminate knock-on electrons from the target, a 12 μm aluminum foil was placed in front of the detector. This protection was found to be essential in maintaining reasonable resolution at the high count rates (~ 15 000/sec) encountered in the present experiment.

In summary, with a bias of 250 V, the annular detector gave 40 keV resolution with a pulser. The best resolution observed at low count rates for 10 MeV protons was 55 keV. During the actual experiment the resolution was 65–70 keV. An additional cooled Si(Li) detector placed at 140° was used for monitoring the beam energy during the run and for normalization of the spectra.

2.3. GERMANIUM DETECTOR

The gamma rays were detected by a lithium-drifted germanium counter of 40 cm^3 intrinsic volume. It was made from a cylindrical pulled crystal by drifting lithium radially toward the center and also axially from one end, to a depth of 13 mm; thus, it was a closed-ended coaxial ("5-sided" coaxial) detector. Fabrication was done at the LRL counter laboratory by R. H. Pehl and co-workers. The detector holder and cooling apparatus were of the standard type and have been described elsewhere.

The measured capacity of the detector was 34 pF. At the usual operating bias of 2000 V, it was capable of 2.4 keV resolution for ^{60}Co (1.33 MeV gamma). The full energy (FE) peak height to Compton edge height was ~ 20 to 1. When the detector was placed in the experimental cave, the best resolution obtained was 4 keV. The increase was mainly to be due to noise pick-up in the transmission lines between

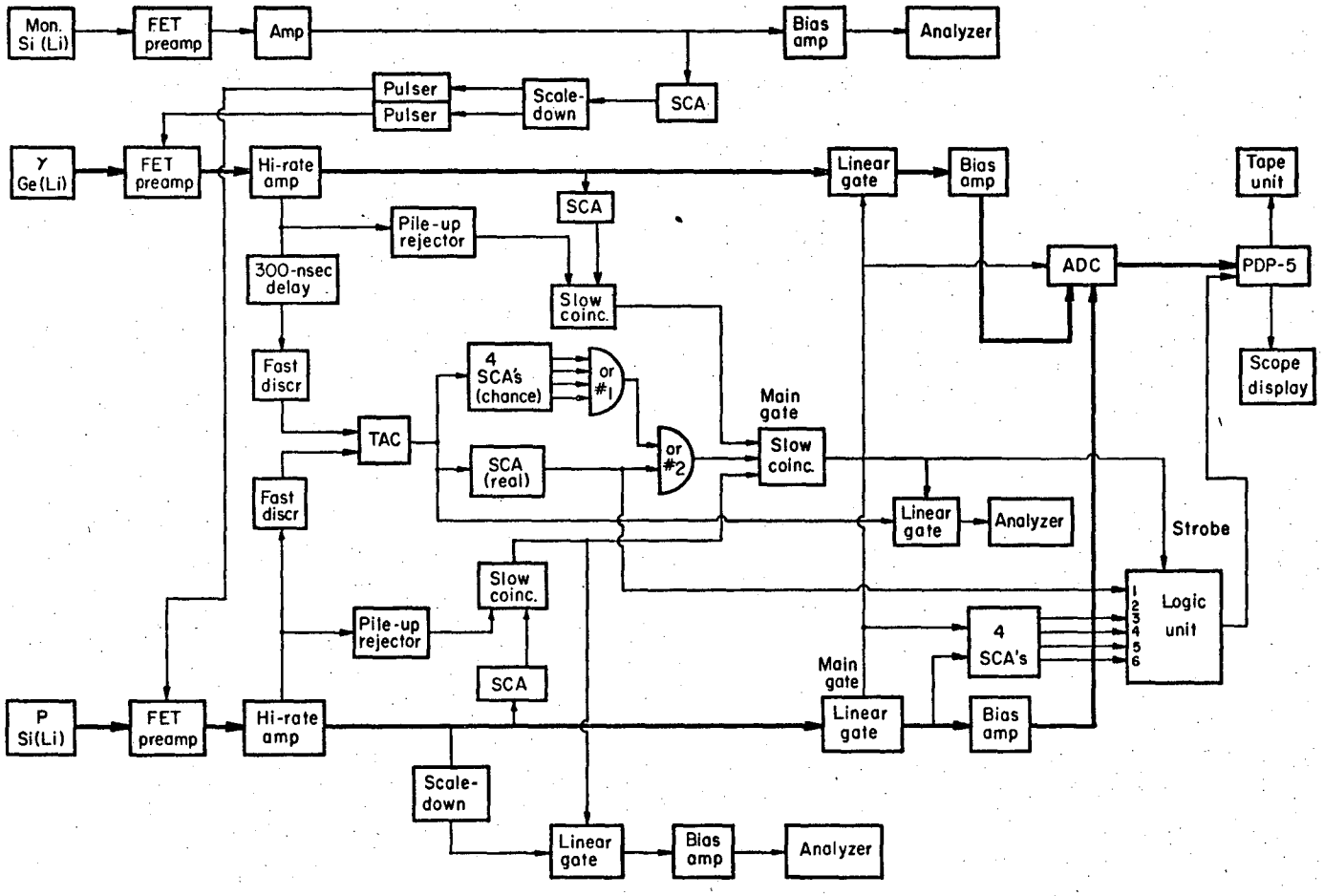

Fig. 1. Block diagram of the electronics for the ^{54}Fe spectroscopy experiment. The heavy lines indicate the paths of the energy signals from the two detectors.

the experimental and counting areas. During the experiment, the observed resolution was ~ 6 keV for 1 MeV γ-rays; the additional increase was due to high counting rates (~ 20 kHz), and small gain drifts encountered during runs. No gain shifts as large as 1 keV were observed. Calibration of the Ge(Li) detector was accomplished using a set of IAEE † calibrated sources; the relative efficiency above 1.8 MeV was obtained using a ^{56}Co source.

2.4. ELECTRONICS

Fig. 1 shows a simplified block diagram of the electronics system. A nearly identical system is described in detail in ref. [16]), thus we will repeat here only a few of the more pertinent details.

The central features of both proton and gamma counter electronics are the Goulding, Landis and Pehl high-rate amplifier systems [17]). These systems employ pole-zero cancellation to eliminate base-line undershoot, and pile-up rejection to insure that, any signal whose amplitude is changed due to the proximity of another signal, is not stored.

Leading edge timing was used for both detectors. The outputs of fast discriminators were fed into a time-to-amplitude converter (TAC); the latter provided the required information on the time correlation between any two pulses. Sections of the TAC spectrum containing either real and chance events or only chance events were used to generate logic signals which opened linear gates in both the gamma and proton systems. The logic signals along with the gated energy signals were fed into a multiplexed 4096-channel ADC, and subsequently into an on-line PDP-5 computer.

The on-line program chose a portion of the coincidence array for an oscilloscope display and, in addition, stored the entire array, event by event, on magnetic tape. The stored data thus consisted of two numbers characterizing the proton and gamma energy signals and a logic bit which indicated whether the event was from the real plus chance or chance portion of the time spectrum. After completion of the experiment, the coincidence spectra were constructed by computer analysis of the magnetic tape.

3. Experiment and analysis

3.1. EXCITATION FUNCTION

Previous experiments on ^{54}Fe at this laboratory had indicated that inelastic cross sections for the ^{54}Fe(p, p′) reaction varied quite strongly with energy in the region around 9 MeV incident proton energy. For this reason, prior to performing the coincidence experiment, the excitation function for this reaction was measured in steps of 100 and 200 keV from 8 to 13 MeV. For the experiment, the high resolution experimental area described in ref. [18]) was used. Fig. 2 shows the results of the experiment from 8.5 to 10.5 MeV for states up to 4.287 MeV.

† Sources obtained from the International Atomic Energy Agency.

Changes in inelastic cross section due to small shifts in beam energy during the coincidence run could have produced errors in normalization. It was, therefore, important to choose a beam energy where the excitation function was reasonably flat, thereby minimizing the variation of cross section with energy. It is apparent from fig. 2 that this criterion could not be met simultaneously for all states; however, it was felt that 10 MeV was a good compromise for most of them.

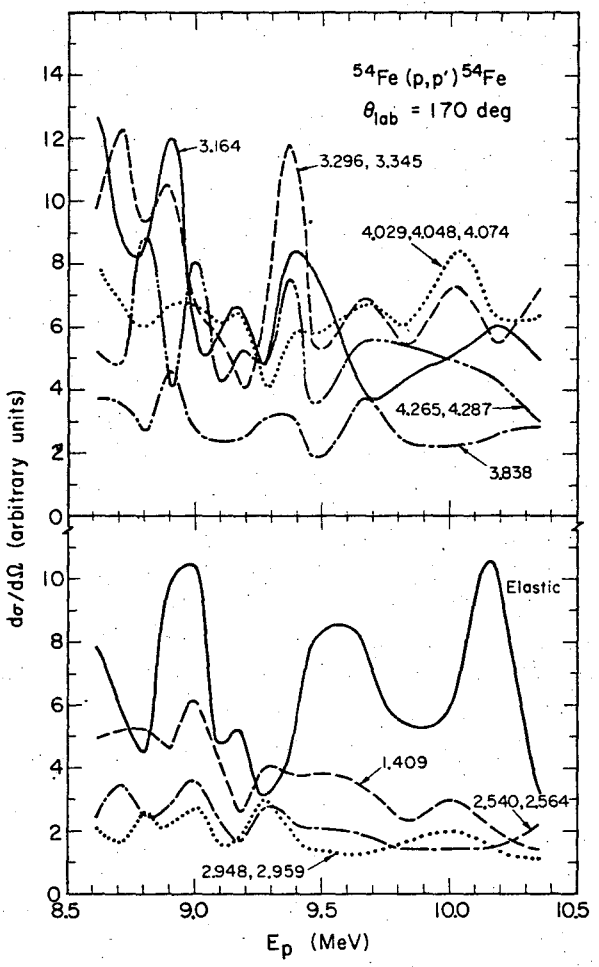

Fig. 2. Excitation functions for various states in the reaction ^{54}Fe(p, p')^{54}Fe from 8.5 to 10.5 MeV. The differential cross sections were measured at 170° lab. angle in steps of 100 keV and 200 keV.

3.2. COINCIDENCE EXPERIMENT

The intensity of γ-rays, in coincidence with inelastically scattered protons detected in the range 168° to 172°, was measured at 90°, 70°, 55°, 40°, and 25°, with respect to the beam axis. The total data acquisition time at each angle was about 10 h.

This was obtained by summing the counts from seven separate cycles through the angular range. By taking a series of short runs at each angle and subsequently combining them, it was hoped to further reduce the effect of any normalization error due to beam-energy fluctuations.

Various cyclotron parameters were carefully maintained at constant values to insure that no shifts in beam energy occurred. The beam energy was monitored by periodically checking the peak positions in both the monitor and annular-counter spectra. Within the sensitivity of this method, no energy shifts greater than 10 keV were observed during the run. Both proton singles spectra were also checked for variations in the number of inelastic counts per μC; this quantity was constant to within 2 %.

Beam intensities, which were usually about 50 to 60 nA, produced counting rates of $\sim$ 20 000 Hz in the gamma detector and $\sim$ 15 000 Hz in the annular Si(Li) detector. The total rate of real coincidences was about 25 Hz.

3.3. ANALYSIS

3.3.1. Angular correlations. The analysis was accomplished by summing the coincidence array over all γ-ray energies to produce real and random proton coincidence spectra. Gamma coincidence spectra were then generated for each peak which was cleanly resolved in the proton spectrum. Summation of the peaks in the γ-coincidence spectra varied considerably, depending on the complexity of the spectrum. For spectra generated from well-separated states in the proton spectrum, the γ-summation for the highest energy transition included the FE peak, escape peaks (if any), and Compton distribution. This procedure was used only in cases where it was clearly justified, and in all cases, the results were checked against the corresponding FE-peak summations. For lower-energy γ-rays in simple spectra, and in the case of more complicated spectra, only peak summation was used. In these cases, where necessary, an average background was evaluated by summing a few channels on either side of the peak and subtracted out.

For states which were not cleanly resolved in the proton spectrum, the total number of γ-ray counts was obtained by summing the appropriate FE-peak region in all spectra which contained counts due to the given state.

The spectra were normalized to the total charge collected on the Faraday cup. Equivalently, the total number of monitor counts could have been used, since the two methods yielded identical results within 1.5 to 2 %. The dead-time and pile-up rejection losses were accounted for in the manner discussed in ref. [16]).

Errors. Since accurate error evaluation is essential to the spin assignment arguments given in subsect. 4.2, great care was taken to eliminate systematic errors from the present analysis. For the highest-energy γ-ray transitions, no background (i.e., real coincident background) was present and the errors quoted are those due to the uncertainties in the number of counts and in the number of chance counts subtracted. When background subtraction was necessary, only the statistical errors from the

background evaluation were combined with those above. In some cases, it was advantageous to subtract the Compton background from the cascade $2_1^+ \rightarrow 0_1^+$ transition (present in all spectra). This was possible since the pure $2_1^+ \rightarrow 0_1^+$ spectrum was available. All statistical errors propagated by this procedure were included.

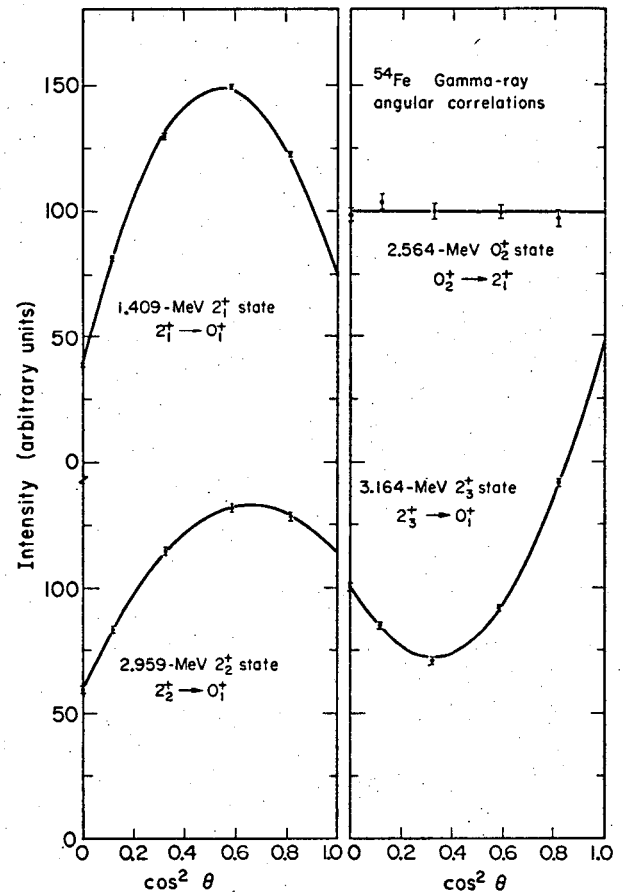

Fig. 3. (a) Theoretical fits, assuming $J_i = 2$ and $J_f = 0$, to the experimental angular correlations for the 1.409 MeV state (1.409 MeV γ-ray) and the 2.959 MeV state (2.959 MeV γ-ray). (b) Theoretical fits to the experimental angular correlations for the 2.564 MeV state (1.155 MeV γ-ray) assuming $J_i = 0$, and for the 3.164 MeV state (3.164 MeV γ-ray) assuming $J_i = 2$ and $J_f = 0$.

Fortunately, there existed a method of checking the assumption that statistical errors were dominant in the present analysis. The 2.564 MeV state was determined to be a 0^+ by Church *et al.* [19]); therefore, the observed $0_2^+ \rightarrow 2_1^+$ transition must be isotropic. As is seen in fig. 3, a fit to the experimental angular distribution using only an isotropic term is consistent within the errors, which are $\sim 2.8\,\%$. Further checks were obtained by fitting the ground-state transitions for the known 2^+ states at 1.409, 2.959 and 3.164 MeV with theoretical $2^+ \rightarrow 0^+$ curves from eq. (5); these are shown in

fig. 3. The χ^2 obtained for the 2.959 and 3.164 MeV states are reasonable (respective average errors on the points were 1.4 % and 1.1 %). However, χ^2 obtained for the 1.409 MeV state suggests that an additional error of about 1 % may be present; this was necessary to reduce χ^2 to the 50 % confidence level; the statistical errors ranged from 1.6 % at 90° to 0.66 % at 40°. The effect of such an error would be quite small on any of the other angular distributions. It appears, then, on the basis of this evidence, that the assumption of negligible normalization error is justified.

Method of analysis. The method of analysis used is quite similar to that of Poletti and Warburton [9]). Eq. (1) may be written as

$$W_{\mathrm{T}}(\theta) = \sum_k [\rho_k(a, 0)I(0)+\rho_k(a, 1)I(1)]F_k(ab)Q_kP_k(\cos\theta), \tag{5}$$

where

$$P(0) = I(0)/(I(0)+I(1)) \quad \text{and} \quad P(1) = I(1)/(I(0)+I(1)).$$

For assumed initial and final spins, the unknown parameters of eq. (5) are δ, $I(0)$, $I(1)$; the I's are constrained to be positive. The multipole mixing ratio, δ, enters the F coefficients quadratically, however, a linear least-squares procedure may be used if δ is not considered to be a continuous variable. χ^2 is then minimized with respect to $I(0)$ and $I(1)$ for a range of values of δ and χ^2 is defined as

$$\chi^2 = \frac{1}{n}\sum_{i=1,n}\left(\frac{W_{\mathrm{T}}(\theta_i)-W_{\mathrm{E}}(\theta_i)}{\sigma_i}\right)^2, \tag{6}$$

where n is the number of degrees of freedom; in the present case, it was the number of data points minus two. Equation 5 was evaluated for values of δ in steps of arctan $\delta = 1$ from $-90°$ to 90°.

We have adopted the standard method of explicitly displaying the dependence of χ^2 on δ by plotting χ^2 versus arctan δ. These curves showed solutions for certain values of δ for at least one of the spin combinations. Accepted solutions were those exhibiting a χ^2 within the range expected for $n-2$ degrees of freedom as given by the χ^2 probability tables [20]). Spins which did not give solutions below the 1 % confidence level were assumed to be incorrect.

In most cases, it was possible to obtain statistically significant angular distributions for more than one γ-ray from a given state; these consisted of either two branch decays from the state or two γ-rays in cascade. In such cases, χ^2 was minimized with respect to all the transitions simultaneously.

In the simultaneous analysis of more than one angular distribution, it was necessary to normalize the curves to a common total intensity. This was done by first fitting the curves individually with the expansion [9]):

$$W(\theta) = A_0+A_2Q_2P_2(\cos\theta)+A_4Q_4P_4(\cos\theta), \tag{7}$$

then dividing the data points by A_0. In the subsequent analysis, it was possible to vary the mixing ratio of only one transition at a time; the others were fixed at an

assumed value. In such cases, several runs were made, in which the mixing ratio considered the variable was changed. This was necessary to eliminate the possibility of missing any minima.

Population of $m > 1$ substates. Litherland and Ferguson [8]) have considered the effect of the finite size of the annular detector on population of $|m| \geqq 2$ substates. On the basis of their work, we have estimated the population of $|m| = 2$ substates to be on the order of 3 % and that of $|m| > 2$ to be negligible. In order to determine the effect of $|m| = 2$ substate population, all fitting was done twice; once with $P(2) = 0$, and once with $P(2) = 0.1\,P(1)$. In most cases, the two calculations were quite similar and in no case were additional spin solutions obtained with the latter calculation.

Multipole mixing ratios. It has become common practice to evaluate the errors for multipole mixing ratios by the following procedure. The point where the χ^2 curve reaches a minimum is normalized to the 50 % confidence level. The two error limits are then given by the points at which the curve crosses the 10 % confidence level. This procedure has the advantage of eliminating the dependence of the quoted errors on the absolute value of χ^2 determined in the fitting. The additional uncertainty incurred by population of $|m| \geqq 2$ substates has been included by some authors [9]). However, we have found this effect to be negligible; therefore, only the errors evaluated by the first method are given in the present analysis.

3.3.2. Doppler-shift analysis. The usual procedure in measuring an attenuated Doppler shift is to observe the γ-ray energy at two widely separated angles. The maximum shift in this case is given by

$$\Delta E_{\max} = \frac{v_0}{c}(\cos\theta_1 - \cos\theta_2)E_0. \tag{8}$$

In the present experiment, the angular range spanned was only from 25° to 90°. However, the precision with which the centroid shift could be determined was increased by evaluating the centroid of the peak at all five angles. A least-squares minimization was then used to calculate a line of the form $E_0 + \Delta E_{\mathrm{obs}}(\cos\theta)$. The ΔE_{obs} given in the following discussion is listed in terms of $E_{25°} - E_{90°}$. The errors in ΔE_{obs} were obtained by combining the statistical errors from the centroid evaluations with an estimate of the error due to the uncertainty in the region over which to evaluate the centroids. These estimates were in general agreement with those inferred from the least-squares fit.

To obtain $\Delta E_{\max}$, the initial recoil velocity v_0 was calculated from kinematics of the reaction for each state. This quantity was then averaged over the angular acceptance of the annular counter. Further effects due to the finite size of both counters were estimated to be about 1 % and were therefore neglected.

As was discussed in subsect. 1.3, in order to relate the measured attenuation factor, $\Delta E_{\mathrm{obs}}/\Delta E_{\max}$, to the quantity $F(\tau)$ from eq. (5), it is necessary to know $\mathrm{d}E/\mathrm{d}x$ through-

out the range of velocities. We have used the form:

$$dE/dx = k_e v + (dE/dx)_n. \tag{9}$$

The first term is the electronic contribution to the stopping power, which in the theory of Lindhard, Scharf and Schiøtt [15]) (LSS), is proportional to the velocity of the ion. The compilation of data by Northcliffe [21]) shows that in the velocity range $v/c \leqq 137$, this form for the electronic stopping is accurate, but that the values of k_e predicted by LSS are systematically about 20 % too low. No data were analyzed however, for ions as heavy as ^{54}Fe.

Eswaran *et al.* [22]) have measured the lifetimes of states in ^{56}Fe, ^{62}Ni, and several isotopes of Cu by the DSAM. They obtain k_e by interpolating from stopping power data on several types of ions in nickel. Their value of k_e for ^{56}Fe is essentially that predicted by LSS. The predicted lifetime of the first 2^+ state in ^{56}Fe agrees well with that obtained from other methods.

A more recent analysis of heavy-ion stopping data has been given by Steward and Wallace [23]). Their work included some of the data analyzed by Northcliffe and, additionally, fission fragment range data. On the basis of their systematics, the value of k_e for ^{54}Fe ions stopping in ^{54}Fe is 12 % higher than that of LSS. We have chosen to use this latter estimate of k_e in the present analysis.

The predicted curve of the nuclear stopping power $(dE/dx)_n$ has not been tested directly by experiment. We have therefore adopted a functional form, given in ref. [23]) which fits $(dE/dx)_n$ given by LSS. In the Thomas-Fermi units of energy and distance (see refs. [12, 15])):

$$(d\varepsilon/d\rho)_n = 4.57\varepsilon^{\frac{1}{2}} \exp(-2.54\varepsilon^{0.277}). \tag{10}$$

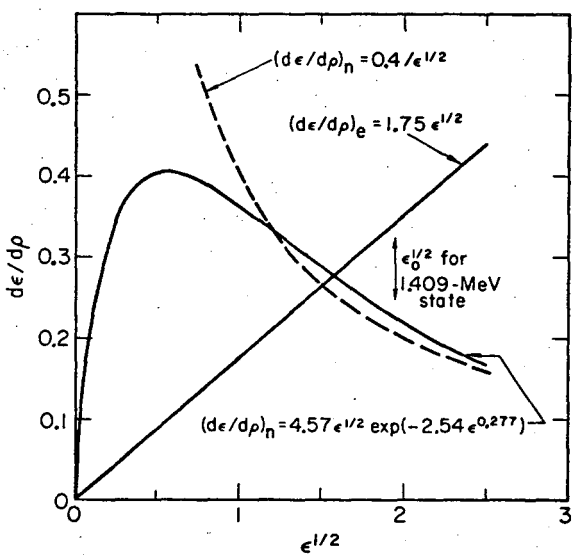

Fig. 4. Stopping power $(d\varepsilon/d\rho)$ versus velocity $(\varepsilon^{\frac{1}{2}})$ both in Thomas-Fermi units. Shown are the electronic stopping power and two functional forms which approximate the nuclear stopping power.

Some calculations were also made using the form:

$$(\mathrm{d}E/\mathrm{d}x)_n = 0.4/\varepsilon^{\frac{1}{2}}. \tag{11}$$

In the present analysis, it made little difference in $F(\tau)$ whether eq. (10) or (11) was used. Fig. 4 shows the nuclear and electronic stopping powers over the relevant velocity range for the present experiment. We have included an estimated 10 % error in $F(\tau)$, resulting from the lack of knowledge of $\mathrm{d}E/\mathrm{d}x$. The errors in the mean lifetimes are thus a combination of the uncertainties in $\Delta E/\Delta E_0$ and in $F(\tau)$.

The range of the recoils predicted from the total $\mathrm{d}E/\mathrm{d}x$ was ≈ 160 g/cm^2, which is a sizeable fraction of the target thickness of 837 g/cm^2. Thus it was necessary to correct the predicted $F(\tau)$ for those ions which escaped from the target. This was done by constructing a curve of distance versus time. Then for recoils within the total range of the back of the target, eq. (4) was integrated out to a time t_e at which the recoil escaped from the target; in the remaining integration $v(t)$ and $\cos\phi(t)$ were constant at the values $v(t_e)$ and $\cos\phi(t_e)$, respectively.

Comparison of the lifetimes derived in the present analysis to those obtained from other experiments is given in subsect. 4.2.

4. Results

4.1. OBSERVED STATES

Accurate excitation energies from high-resolution (p, p') experiments on ^{54}Fe have been reported by Aspinall *et al.* [24]) and by Sperduto and Buchner [25]). This

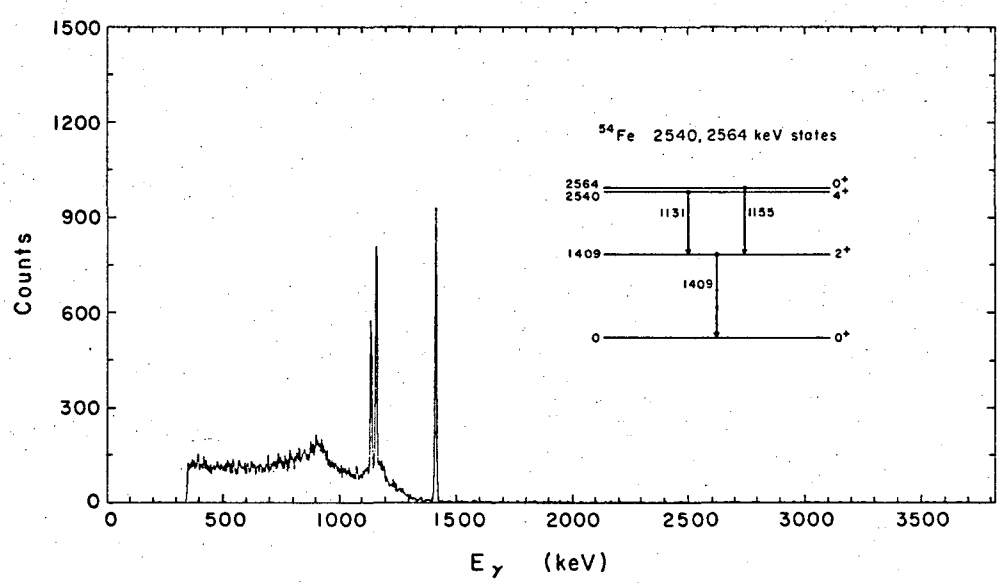

Fig. 5. The γ-ray coincidence spectrum for the 2540, 2564 keV states (unresolved in the proton spectrum) of ^{54}Fe at $\theta_\gamma = 55°$.

information was quite valuable in allowing the unambiguous interpretation of the coincidence spectra.

All levels below 5 MeV which were seen by Aspinall *et al.* were observed in this experiment. Further, the known 6^+ state at 2.948 MeV which was not seen in the high-resolution (p, p′) work was observed here. Sperduto and Buchner [25]) report a level not seen in ref. [24]), which was unresolved from a strong level at 2.540 MeV; the presence of this level was inferred from a peak shape analysis. Hansen *et al.* [26]) have reported levels at 2.537 and 2.550 MeV seen in the ^{54}Fe(d, d′)^{54}Fe reaction at 7.5 MeV. Both states were made with very small cross sections (0.02 and 0.03 mb/sr, respectively). In the present coincidence experiment, we have observed only one level in this energy region at an excitation energy of 2.539 ± 0.001 MeV. The γ-ray coincidence spectrum (fig. 5) reveals no additional transition either to the 1.409 MeV 2_1^+ or to the ground state. (The level at 2.564 MeV, which was unresolved from the 2.539 MeV level in our proton spectrum, was seen in both the (p, p′) and (d, d′) experiments and thus presents no problem.) Furthermore, within the experimental resolution (5 keV), no transition to another state from any higher excited state was observed. In another coincidence spectrum taken at 9 MeV incident proton energy, no evidence was seen of any level but that at 2.539 MeV.

TABLE 1

Comparison of excitation energies for levels of ^{54}Fe (energies in keV)

Present experiment	Sperduto and Buchner; (p, p′) ref. [25 a])	Aspinall *et al.* (p, p′) ref. [24]) a)	Hansen *et al.* (d, d′) ref. [26])	Wegener decay of ^{54m}Co ref. [27])
1408±1	1409±4	1408±4	1410±4	1408±1
	2534±5		2537±6	
2539±1	2540±6	2540±4	2550±6	2537±2
2564±1	2564±5	2563±4	2566±6	
2948±2				2948±3
2961±2	2959±5	2971±4	2959±6	
3163±2	3164±5	3161±4	3167±8	
3298±2	3296±5	3291±4		
3345±2	3345±5	3340±4	3349±8	
3836±2	3838±5	3829±4		
4037±3		4029±4		
4048±2	4048±2	4047±4		
4072±2	4074±5	4070±4		
4271±3		4265±4		
4290±3		4287±4		
4583±2		4579±4		
4655±3		4656±4		
4702±3		4700±4		
4787±3		4781±4		
4950±3		4949±4		

a) Only random errors are quoted for these numbers.

We have identified the 2.539 MeV state as having $J^\pi = 4^+$, which is in agreement with the assignment of Wegener [27]), who observed a 4^+ state at 2.537 ± 0.002 MeV in the decay of ^{54}Co. Since our excitation energy assignments are in general agreement with those of Sperduto and Buechner, their level at 2.540 MeV is probably the 4^+. The evidence for the presence of another level then is somewhat contradictory. We conclude, that if an additional level is present in the region of 2.54 MeV, it is excited in our work with a differential cross section less than 0.005 mb/sr (this is less than 5 % of the 4_1^+ cross section). This applies to angular range 168° to 172° at proton energies of 9 and 10 MeV.

A comparison of the excitation energies from this experiment with those from previous work is shown in table 1. The agreement is generally satisfactory, particularly between our assignments and those of Sperduto and Buechner. In the following discussion for convenience, the energies of transitions from levels below 4.2 MeV are referred to by the energies determined from the numbers of ref. [25]), those above this point are derived from ref. [24]). Thus the excitation energies from our work appear *only* in table 1.

4.2. DETAILED SPECTROSCOPY

This section is devoted to a presentation of the angular correlation and lifetime information obtained for each excited state. In subsect. 4.3, all of the electromagnetic transition data, i.e., lifetimes, multipole mixing and branching ratios, are summarized in tables 2-5. In the summary and in the discussion previous to it, we have referred to electric and magnetic reduced transition strengths in terms of Weisskopf units (W.u.); the values given by Wilkinson [28]) have been used.

1.409 MeV state. The spin of the first-excited state is well known from many experiments. The BE2 of the $2^+ \rightarrow 0^+$ transition has been measured by Coulomb excitation [29]) and by electron scattering [30]) and thus affords a test of the Doppler-shift analysis. A comparison of the BE2's is given below:

Measurement	BE2($e^2 \cdot \mathrm{fm}^4$)
Coulomb excitation	102 ± 4
electron scattering	104 ± 6
Doppler shift	131^{+50}_{-32}

The measured lifetime of 1.1 psec is near the limit of sensitivity of the DSAM, resulting in rather large errors; within the errors the agreement is satisfactory. Using the BE2 from Coulomb excitation, the transition strength is 8.4 W.u. and is thus collectively enhanced.

The 2.540 and 2.564 MeV states. The γ-coincidence spectrum at 55° (all succeeding coincidence spectra illustrated are at this angle) for these states which are unresolved in the proton spectrum, is shown in fig. 5; no evidence is seen for another state in this

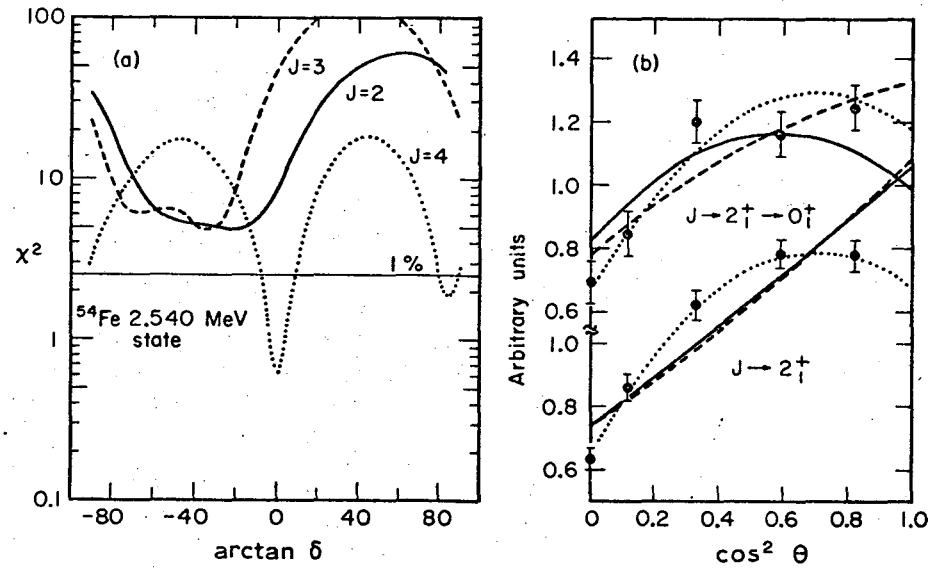

Fig. 6. χ^2 *versus* arctan δ for the 2.540 MeV state of ^{54}Fe and the best fits to the experimental angular correlations for each initial spin. The $J_1 \rightarrow 2_1^+$ and $2_1^+ \rightarrow 0_1^+$ angular correlations were analyzed simultaneously. For a correct spin solution χ^2 should be near unity.

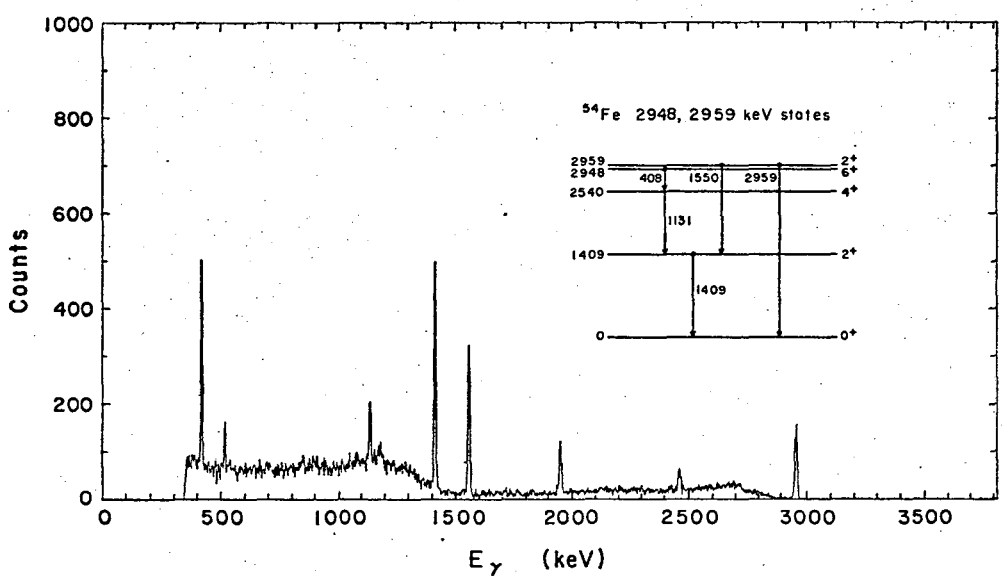

Fig. 7. Gamma-ray coincidence spectrum for the 2948 and 1959 keV states of ^{54}Fe (unresolved in the proton spectrum) at $\theta_\gamma = 55°$.

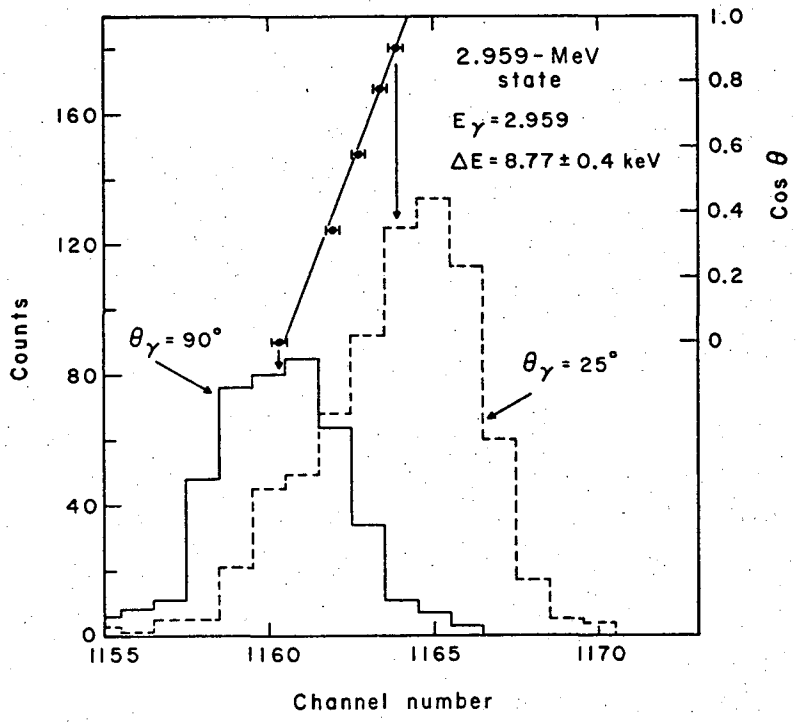

Fig. 8. Summary of the Doppler-shift analysis for the 2.959 MeV state (2.959 MeV γ-ray). The FE γ-ray peaks at $\theta_\gamma = 90°$ and $\theta_\gamma = 25°$ are shown. Shown on the same channel scale is the best fit line to the centroids of all five gamma angles. The form of the line was $E_0 + \Delta E_{obs} \cos \theta_\gamma$.

energy region. On the basis of the decay of ^{54}Co, Sutton *et al.* [31]) first suggested that the 2.540 MeV level was the 4^+ member of the $(f_{\frac{7}{2}})^2$ proton configuration. Several (p, p') and (α, α') experiments are in agreement with this assignment, but are themselves ambiguous in part because of the presence of the unresolvable 2.564 MeV state. More recently, Wegener [27]) re-examined the decay of ^{54m}Co, using (γ, γ) angular correlation techniques and was able to assign J^π of 4^+ to the 2.540 MeV state and J^π of 6^+ to the 2.948 MeV state. The results of the present angular correlation analysis are shown in fig. 6, it is seen that only $J = 4$ gives a solution, thus confirming the assignment of Wegener.

The 2.564 MeV state is known to be a 0^+ from the work of Church *et al.* [19]). This assignment was first suggested by Belote *et al.* [23]). Fig. 3 shows that the angular distribution of the $0^+ \rightarrow 2^+$ γ-ray from this state is isotropic, as expected.

Both the $4_1^+ \rightarrow 2_1^+$ and the $0_2^+ \rightarrow 2_1^+$ γ-rays show very small Doppler shifts, thus it can be said only that their lifetimes are longer than 3 psec and 2 psec, respectively.

The 2.948 and 2.959 MeV states. The coincidence spectrum of these states is shown in fig. 7. The 2.948 MeV state is known to have J^π of 6^+ from the work of Wegener [27]). The angular distributions of $6^+ \rightarrow 4^+$, $4^+ \rightarrow 2^+$ transitions obtained here

were consistent with this assignment, but due to poor statistics, other initial spins also gave solutions.

The 2.959 MeV state was assigned J^π of 2^+ from the work of Thomas *et al.* [7]). The simultaneous fitting of both the 1.550 MeV $2_2^+ \to 2_1^+$ and the 2.959 MeV $2_2^+ \to 0_1^+$ angular distributions from this experiment yielded a value of $\delta(2_2^+ \to 2_1^+) = 0.105^{+}_{-}[^{0.040}_{0.042}]$. This is in reasonable agreement with the value $\delta = 0.25 \pm 0.19$ obtained by Thomas *et al.* [7]). The analysis in the latter reference ruled out a second solution of $\delta = -3.3$, found in the present work.

Fig. 8 shows a summary of the Doppler-shift analysis for the 2.959 MeV level, which gave a mean lifetime of 0.075 ± 0.012 psec; this is an average of the values obtained from the 1.550 and 2.959 MeV γ-rays. Combining the lifetime determination with the branching ratio for the 2.959 MeV transition yields a BE2 of 27.2 ± 4.5 $e^2 \cdot \text{fm}^4$. This is in poor agreement with (e, e') experiment of ref. [30]), where the value 45 ± 5 $e^2 \cdot \text{fm}^4$ was obtained. However, since the resolution in the (e, e') experiment was 700 keV, the 2.959 MeV level was not resolved from the other states nearby and thus the BE2 may be overestimated.

The 3.164 MeV state. This level decays to both the ground state and to the 2_1^+. It has been assigned a J^π of 2^+ by Thomas *et al.* [7]). The mixing ratio for the $2_3^+ \to 2_1^+$ transition is poorly fixed in our analysis, it is clear, however, from the value $\delta = 0.63^{+0.57}_{-0.25}$ that there is strong E2 competition in the transition. The results of the

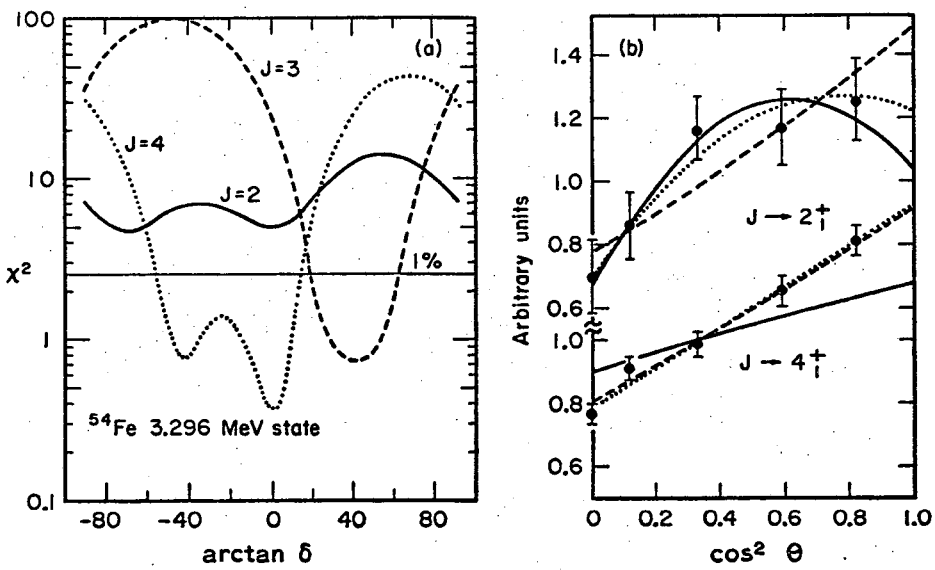

Fig. 9. χ^2 analysis for the 3.296 MeV state of ^{54}Fe and best fits to the experimental angular correlations for each initial spin. The $J_i \to 4_1^+$ and $J_i \to 2_1^+$ angular correlations were fitted simultaneously. The variables displayed explicitly are as follows: for $J_i = 4$, $\delta(4 \to 2) = 0$ and $\delta(4 \to 4)$ is shown; for $J_i = 3$, $\delta(3 \to 2) = -0.55$ and $\delta(3 \to 4)$ is shown; for $J_i = 2$, $\delta(2 \to 4) = 0$ and $\delta(2 \to 2)$ is shown.

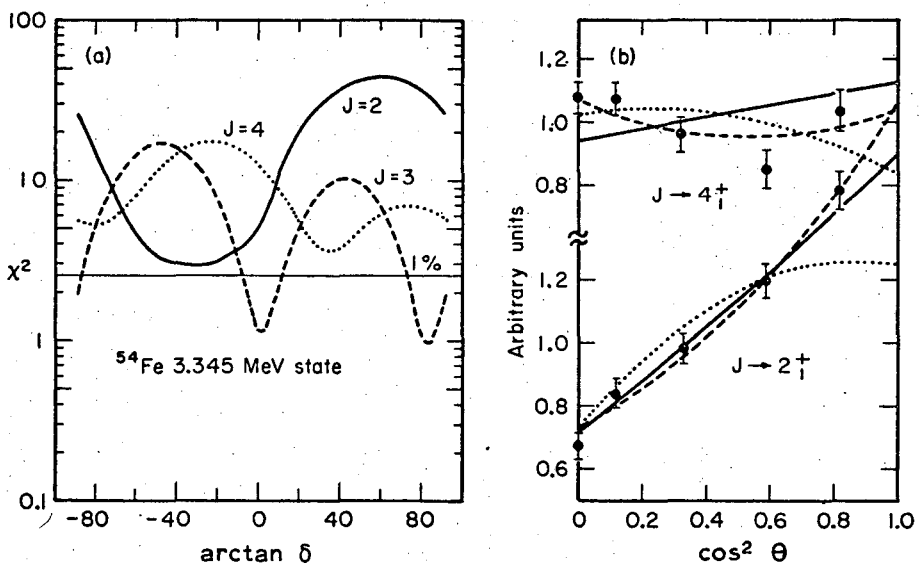

Fig. 10. χ^2 analysis for the 3.345 MeV state of ^{54}Fe and best fits to the angular correlations for each initial spin. The $J_i \rightarrow 4_1^+$, and $J_i \rightarrow 2_1^+$ angular correlations were analyzed simultaneously. The variables displayed explicitly are as follows: for $J_i = 4$, $\delta(4 \rightarrow 2) = 0$ and $\delta(4 \rightarrow 4)$ is shown; for $J_i = 3$, $\delta(3 \rightarrow 2) = -0.8$ and $\delta(3 \rightarrow 4)$ is shown; for $J_i = 2$, $\delta(2 \rightarrow 4) = 0$ and $\delta(2 \rightarrow 2)$ is shown.

Doppler-shift analysis gave a mean lifetime for this level of $0.23^{+0.05}_{-0.04}$ psec. This corresponds to a $2_3^+ \rightarrow 2_1^+$ transition strength which is slightly retarded with respect to the single-particle estimate (0.73 W.u.).

The 3.296 and 3.345 MeV states. These states were unresolved in the proton spectrum. The angular correlation analysis for the 756 MeV and 1887 keV transitions from the 3.296 MeV state is shown in fig. 9. The curves shown are as follows: for $J = 2$ the variable is $\delta(2 \rightarrow 2)$ with $\delta(2 \rightarrow 4) = 0$, for $J = 3$ the variable is $\delta(3 \rightarrow 4)$ with $\delta(3 \rightarrow 2) = -0.55$, and for $J = 4$ the variable displayed is $\delta(4 \rightarrow 4)$, with $\delta(4 \rightarrow 2) = 0$. These curves show the best solutions obtainable for each initial spin; spins less than 2 and greater than 4 were eliminated on the basis of the observed branches to states of spin 2 and 4. It is seen that spin 2 is eliminated, but spins 3 and 4 are allowed. An attempt was made to resolve the ambiguity by including the cascade $4_1^+ \rightarrow 2_1^+$ transition in the analysis. However, since the 3.345 MeV state also decays to the 4_1^+, the uncertainty in subtracting out its contribution to the transition was too large to allow distinction between a $3 \rightarrow 4 \rightarrow 2$ and a $4 \rightarrow 4 \rightarrow 2$ sequence. Furthermore, no transition to this state from higher-lying levels of known spin distinguished between spin of 3 or 4. The Doppler shift of the $3.296 \rightarrow 1.409$ transition was quite small, indicating only that the lifetime of this state is longer than 3 psec.

The results of the angular correlation analysis for he 3.345 MeV state are shown in fig. 10. The following mixing ratios were held constant at the values given: for $J = 2$, $\delta(2 \rightarrow 4) = 0$, for $J = 3$, $\delta(3 \rightarrow 2) = 0.81$, and for $J = 4$, $\delta(4 \rightarrow 2) = 0$.

It is seen that only $J = 3$ gives a reasonable χ^2. The mixing ratio $\delta(3 \rightarrow 4)$ is confined to the values $\delta = 0 \pm 0.14$ or $\delta \geqq 3.5$, while for the $3 \rightarrow 2_1^+$ transition, δ is confined to the range $-2.9 \leqq \delta \leqq -0.45$. A χ^2 below the 1 % limit may be obtained for $J = 2$ if one allows $\delta(2 \rightarrow 4) \leqq -0.04$, however, lifetime (limit set by the fast coincidence

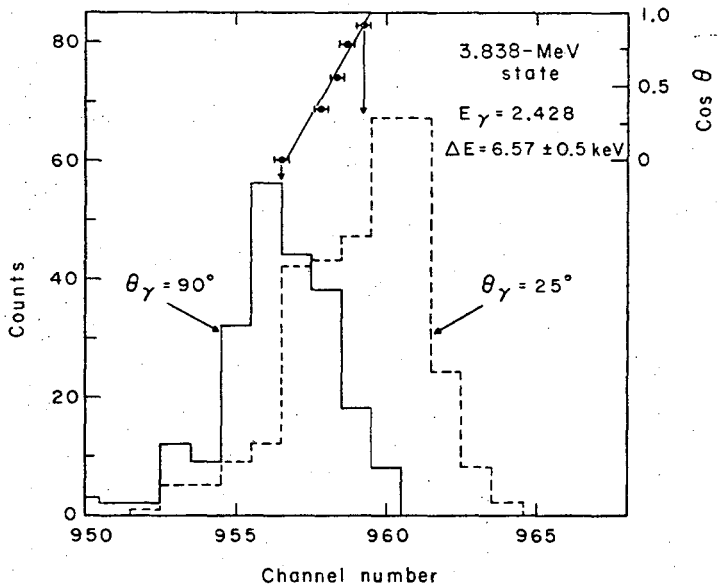

Fig. 11. Summary of the Doppler-shift analysis for the 3.838 MeV state (2.429 MeV γ-ray). The FE γ-ray peaks at $\theta_\gamma = 90°$ and $\theta_\gamma = 25°$ are shown. Shown on the same channel scale is the best fit line to the centroids of all five γ-angles.

resolving time) and branching ratio arguments allow exclusion of any solution requiring a non-zero $\delta(\lambda = 3/\lambda = 2)$. The Doppler-shift analysis for the 3.345 MeV state indicates a lifetime longer than 3 psec.

The 3.838 MeV state. This state has been established as a 4^+ from the work of of Thomas *et al.* [7]). The state decays primarily via E2 radiation to the first 2^+ state, a weak branch is observed to the 2.540 MeV 4^+ state. Only slight evidence was seen for a branch to the 3.296 MeV state found by Thomas *et al.* It was not possible to otbain a mixing ratio for the transition to the 2.540 MeV state, due to poor statistics. The lifetime of the 3.838 MeV level was determined to be 0.091 ± 0.002 psec from the DSAM. This analysis is summarized in fig. 11. A rather large enhancement of 8.0 W.u. is found for the 2.429 MeV E2 transition.

The 4.029, 4.048 and 4.074 MeV states. This triplet was completely unresolved in the proton spectrum. The lowest member of the triplet decays mostly to the 3.296 MeV state, only a weak branch (seen only in the spectrum at $\theta_\gamma = 90°$) is observed to the 4^+ at 2.540 MeV. Due to the spin ambiguity in the final state, the $4.029 \rightarrow 3.296$

MeV, transition does not give an unambiguous spin assignment to the 4.029 MeV level. The possible combinations are:

$J_{4.029}$	$J_{3.296}$
3, 5	4
2, 4	3

On the basis of the observed decays of both states, the combination 4.029(5) → 3.296 (4) is felt to be more likely. The absence of an observable Doppler shift indicates a lifetime longer than 0.6 psec for 4.029 MeV state.

The 4.048 MeV state has strong branch decays to both the 1.409 MeV 2^+ and to the 3.345 MeV 3^+, a very weak branch, seen only at $\theta_\gamma = 90°$, goes to the 2.540 MeV 4^+. The angular distribution analysis of the 703 keV transition indicates spin of either 2 or 4 for this level (the $J \rightarrow 2_1^+$ transition produces no additional information). Using the measured lifetime of $0.44^{+0.34}_{-0.15}$ psec and the branching and mixing ratios, plausible arguments may be given against a $J = 2$ assignment. The lack of an observable ground state decay gives an upper limit of 6 % for the branching ratio. This gives a partial lifetime of 7.3 psec for the ground state decay, corresponding to an E2 transition of $\leqq 0.01$ W.u. Such a decay is considerably more retarded than any observed E2 transition in ^{54}Fe (see table 5). (An M2 $2^- \rightarrow 0^+$ transition is unlikely because of the large mixing ratios observed in the other transitions.) Further evidence against a 2^+ assignment comes from the large mixing ratio observed for an assumed $2^+ \rightarrow 3^+$ transition. This gives a BE2 $\geqq$ 26 W.u., whereas a $4^+ \rightarrow 3^+$ transition is

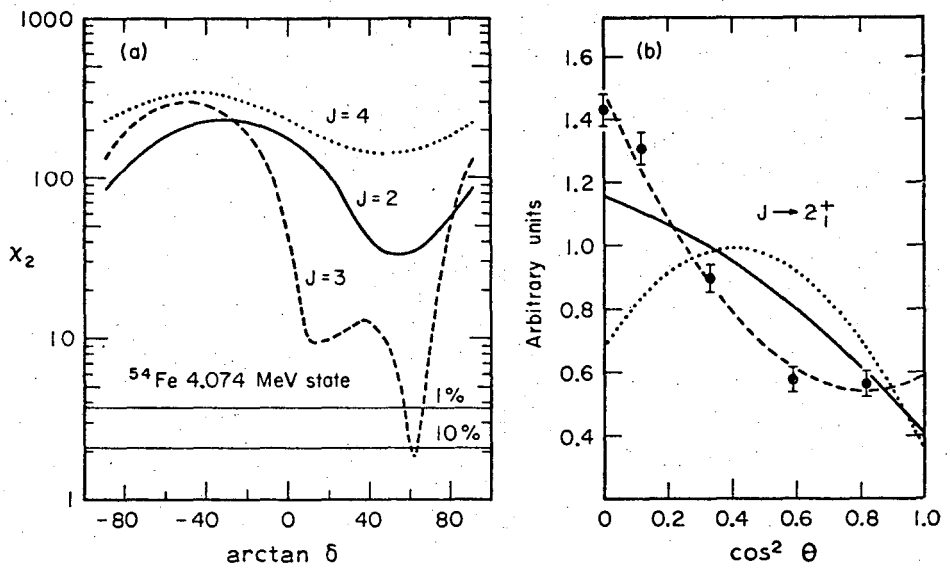

Fig. 12. χ^2 analysis for the 4.074 MeV state. The angular correlation of the 4.074 → 1.409 (2.665 MeV) γ-ray was fitted.

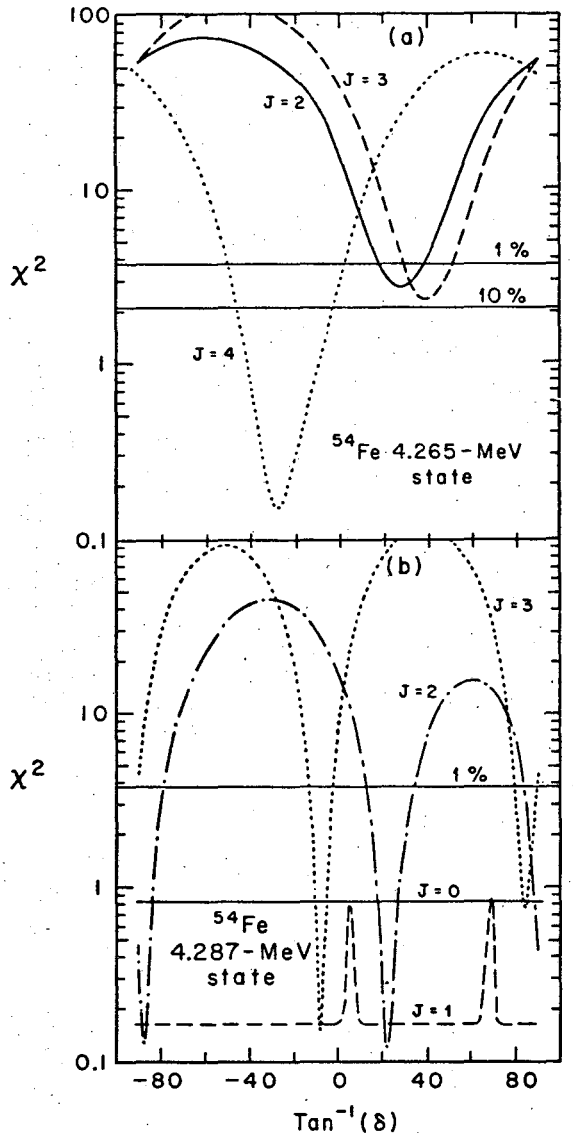

Fig. 13. (a) χ^2 analysis for the transition to the 2_1^+ state from the 4.265 MeV state, (b) χ^2 analysis for the transition to the 2_1^+ state from the 4.287 MeV state.

consistent with a more moderate BE2 (see table 5). Such arguments do not, of course, eliminate $J = 2$ rigorously, however the evidence definitely favors $J = 4$.

The angular correlation analysis for the 4.074 to 1.408 MeV transition gives an unambiguous assignment of $J = 3^{(+)}$ to the 4.074 MeV state (fig. 12). Assuming positive parity, the mixing ratio δ(E2/M1) is $1.88^{+0.50}_{-0.44}$. The $3^{(+)}$ to 4^+ transition is

too weak to provide further information. Using the DSAM, the lifetime of this state was found to be 0.084 ± 0.025 psec.

The 4.265 and 4.287 MeV states. These two states were unresolved in the proton spectrum. The analysis for the 4.265 MeV state is shown in fig. 13(a), only the 1725 keV (4.287 → 2.540) transition was fitted. The cascade transition from the 4_1^+ could not be evaluated without large errors from background subtraction. $J = 2$ is rigorously eliminated because of the non-zero $\delta(\lambda = 3/\lambda = 2)$ required for a reasonable χ^2. Both $J = 4$ and $J = 3$ give χ's below the limit, however, the latter gives a rather poor fit and is thus less likely than $J = 4$. The observed Doppler shift of the 1725 keV transition gave a mean lifetime of $0.119^{+0.033}_{-0.025}$ psec for this level.

The 4.287 MeV level decays entirely to the first 2^+ state, the angular distribution of the transition is, within errors, isotropic, indicating a spin of 0. However, as may be seen in fig. 13(b), spins of $J = 1$, 2, and 3 are not eliminated by the χ^2 analysis, in particular $J = 1$ can give a perfectly isotropic distribution, since the $m = 0$ and $m = \pm 1$ substates can be equally populated. Again, one must appeal to plausibility arguments in order to determine the most likely spin. The measured lifetime and the upper limit of 8 % for a transition to the ground state give the transition probabilities of 0.05 W.u. for a $2_e^+ \rightarrow 0^+$ (E2) decay and 5×10^{-4} W.u. for a $1^+ \rightarrow 0^+$ (M1) decay, both numbers are outside the observed range for this nucleus. Additional evidence for the assignment of $J = 0$ comes from the observed purity of the decay (i.e., only the $J \rightarrow 2_1^+$ transition is seen).

The 4.579, 4.656 and 4.700 MeV states. Limits were set in the proton spectrum to

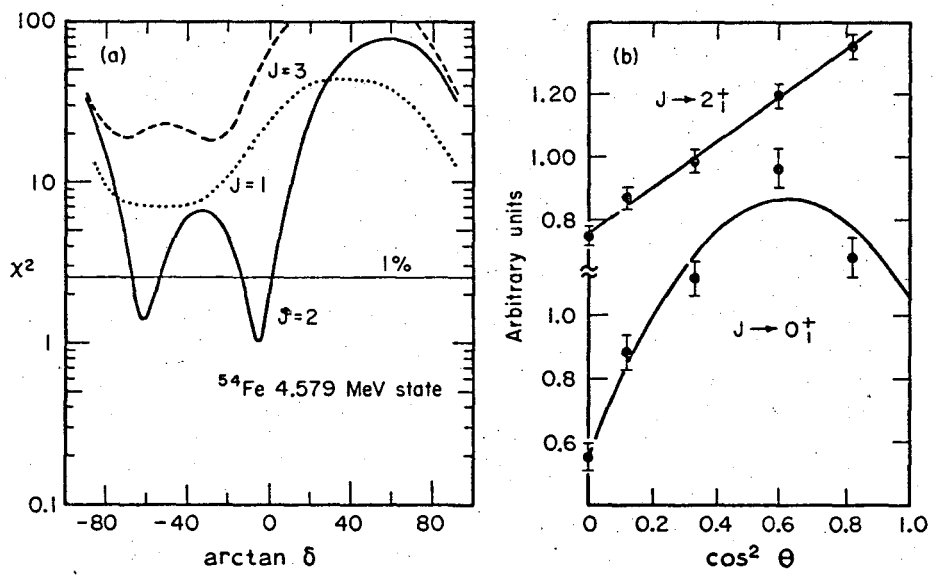

Fig. 14. χ^2 analysis for the 4.579 MeV state. The transitions to the 2_1^+ and to the ground state were analyzed simultaneously.

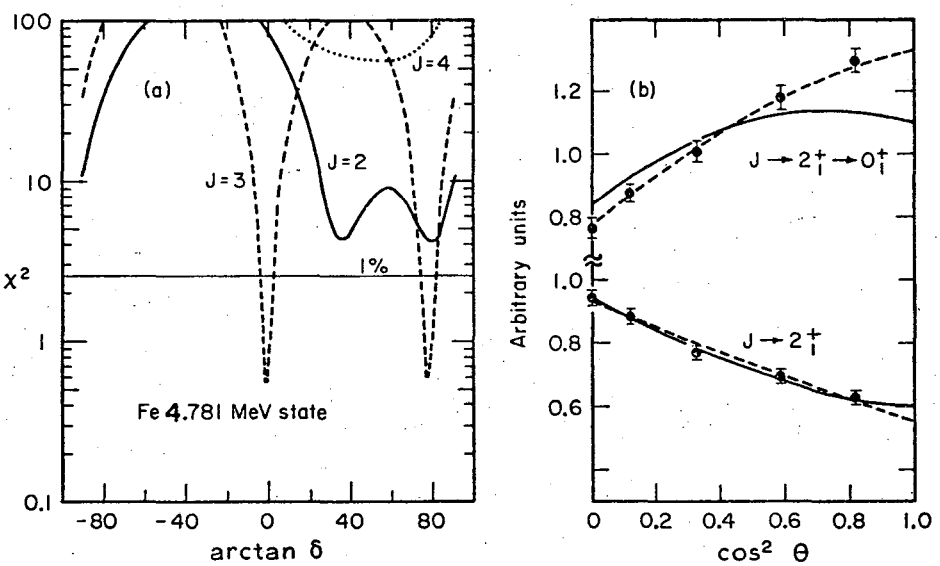

Fig. 15. χ^2 analysis for the 4.781 MeV state. The 4.781 $\rightarrow 2_1^+$ and $2_1^+ \rightarrow 0_1^+$ cascade transitions were fitted simultaneously.

encompass most of this triplet, however there was some contribution of the 4.700 MeV state in two different γ-spectra. The 4.579 MeV level was assigned J^π of 2^+ by Peterson [6]), using the $^{54}Fe(\alpha, \alpha')^{54}Fe$ reaction. From fig. 14 it is seen that $J = 2$ is uniquely determined by analysis of the transitions from this state to the 0_1^+ and 2_1^+ states. Because the double-escape peak efficiency at 4.579 MeV is not well known, the error in the branching ratios for the two transitions is rather large. The observed Doppler shift for this state is, within errors, the maximum possible shift, thus the lifetime is $\leqq 0.01$ psec. The mixing ratio for the 2^+ to 2_1^+ transition is either $\delta = -0.105 \pm 0.09$ or $\delta = -1.8^{+0.4}_{-0.5}$.

Within the present limit of sensitivity, the 4.656 MeV state decays only to the 3.296 MeV state, the 4.700 MeV state decays mostly to the 3.345 MeV $3^{(+)}$ state, with some evidence of a weak branch to the 2.540 MeV 4^+ state. The energies of the two strong γ-rays from these states are within 5 keV and are hence unresolvable. Thus, very little can be inferred about these levels, they are probably of rather high spin ($\geqq 4$).

The 4.781 MeV state. Bellicard and Barreau [30]) have assigned J^π of 3^- to the 4.781 MeV level from electron scattering work. Several other (α, α') [ref. [6])] and (p, p') [refs. [2-5])] experiments have confirmed this choice. However, all these experiments depend upon a reaction model for interpretation. Thus, it was important to determine the spin of this state in a model-independent way. Fitting only the 4.781 $\rightarrow$ 1.409 transition rules out spin 4, but both $J = 2$ and $J = 3$ are allowed. However, when the cascade $2_1^+ \rightarrow 0_1^+$ transition is included (see fig. 15), only $J = 3$

gives a solution, the value of $\delta = 0$ is quite consistent with negative parity for this level. Because of the complex decay of the 3^- state, it was necessary to correct the $2_1^+ \rightarrow 0_1^+$ cascade transition for contributions other than $3 \rightarrow 2 \rightarrow 0$. This could be done because most of the other contribution came from cascades through the 4_1^+ state.

From the properties of cascades of the type $4^{+\gamma 1} \rightarrow 2^{+\gamma 2} \rightarrow 0^+$, it is known the $\gamma 1$ and $\gamma 2$ have identical angular correlations and thus such contributions to the $2^+ \rightarrow 0^+$ decay could be subtracted. All but 10 % of the required correction could be made in this manner, the remainder was felt to be negligible.

The Doppler-shift analysis for both the FE and double-escape peaks of the 3.372 MeV γ-ray gives a mean lifetime of 0.048 ± 0.016 psec for this state. This corresponds to a very retarded BE1 of 1.99×10^{-4} W.u. for the $3^- \rightarrow 2^+$ transition.

The 4.949 MeV state. Although it is weakly excited and thus not visible in the singles proton spectrum, the 4.949 MeV level is cleanly separated in the coincidence array. Decay modes are seen to the 2_1^+, 4_1^+, and 6_1^+ states. The decay mode of the 4.949 MeV state is sufficient to assign it as $J = 4$, this is in agreement with the angular correlation analysis (fig. 16). In fig. 16, the mixing ratios are as follows: For $J = 2$, $\delta(2 \rightarrow 4) = 0$, $\delta(2 \rightarrow 2)$ is the variable, for $J = 3$, $\delta(3 \rightarrow 2)$ is optimized at -0.53 and $\delta(3 \rightarrow 4)$ is the variable for $J = 4$, $\delta(4 \rightarrow 2) = 0$, and $\delta(4 \rightarrow 4)$ is the variable. The $4^{(+)} \rightarrow 4_1^+$ mixing ratio is found to be $= 0.36^{+0.20}_{-0.29}$. The Doppler shift of the 2.409 MeV γ-ray yielded a mean lifetime of 0.042 ± 0.015 psec.

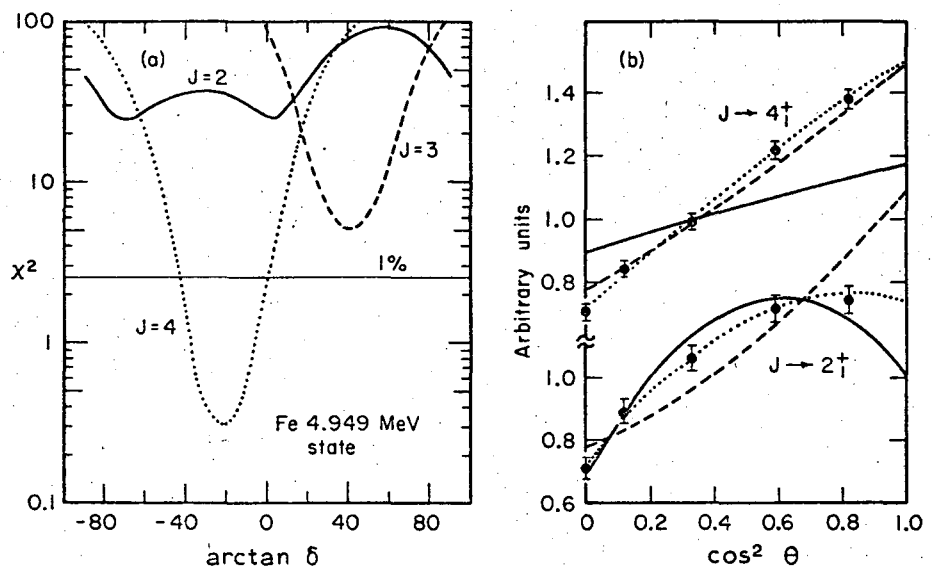

Fig. 16. χ^2 analysis for the 4.949 MeV state. The $4.949 \rightarrow 2_1^+$ and $4.949 \rightarrow 4_1^+$ transitions were fitted simultaneously. The mixing ratios for the assumed initial spins are as follows: for $J_i = 2$, $\delta(2 \rightarrow 4_1^+) = 0$ and $\delta(2 \rightarrow 2^+)$ is the variable; for $J_i = 3$, $\delta(3 \rightarrow 2_1^+) = -0.53$ and $\delta(3 \rightarrow 4)$ is the variable; and the $J_i = 4$, $\delta(4 \rightarrow 2_1^+) = 0$ and $\delta(4 \rightarrow 4_1^+)$ is the variable.

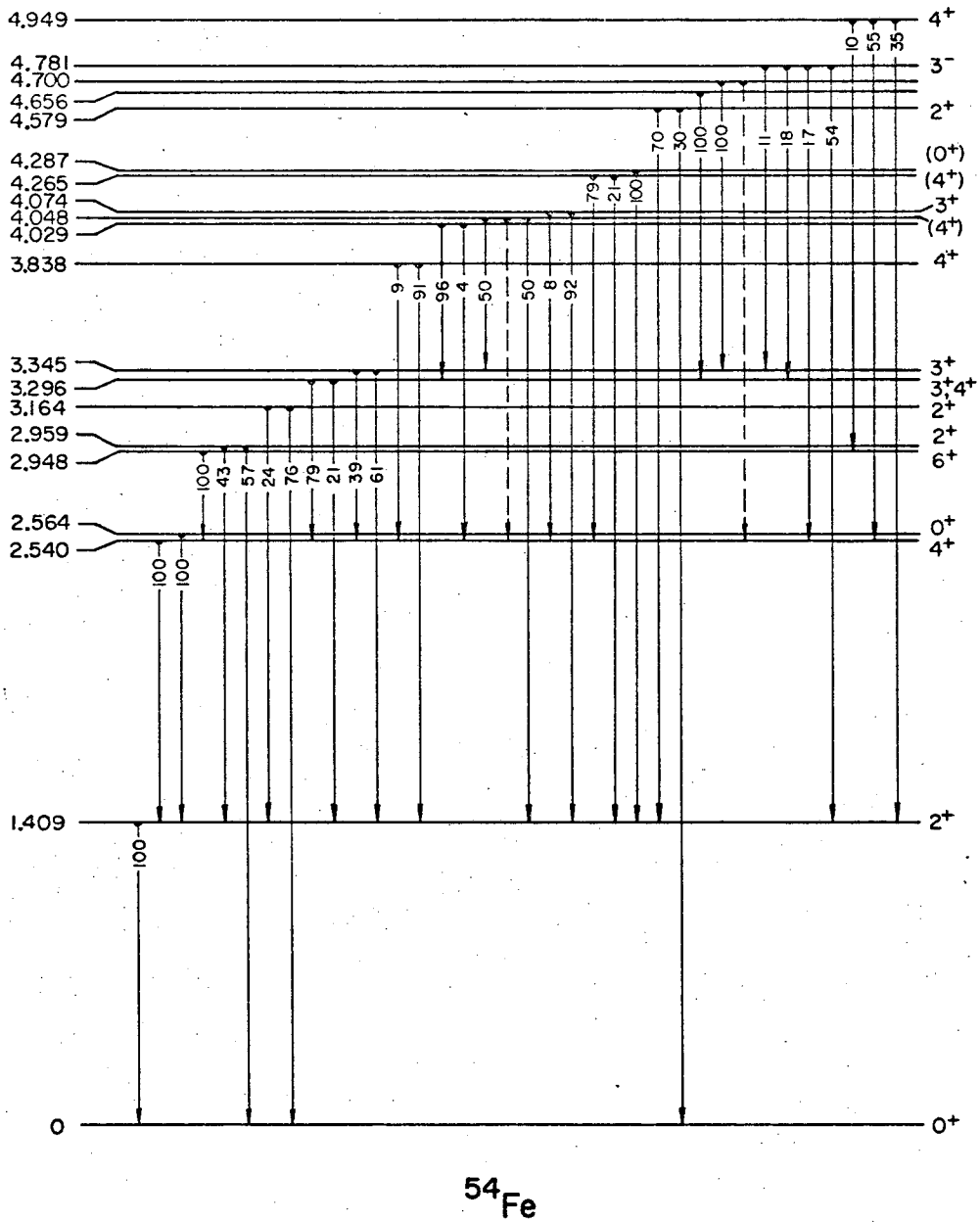

Fig. 17. Levels of ^{54}Fe below 5 MeV. The branching ratios were derived in the present experiment. The spin assignments include those from previous work and from this experiment. The excitation energies are from refs. [24,25]).

Summary of electromagnetic transition data. Fig. 17 summarizes the spin and decay information on levels of ^{54}Fe below 5 MeV, spin assignments from previous experiments are included. The branching ratio and multipole mixing ratio data are summarized in tables 2 and 3. All transitions in which the minimum $|J_i - J_f| = 2$ had mixing ratios which were consistent with zero and hence are not listed in table 3.

The agreement of the branching ratios determined here with those from other experiments is only fair, but within errors. There appears to be strong disagreement,

TABLE 2

Branching ratios for the decay of excited states of ^{54}Fe

Level	E_γ (MeV)	$J_i \to J_f$	Branching ratios	Other values	
				[a]	[b]
1.409	1.409	$2 \to 0$	100		
2.540	1.131	$4 \to 2$	100		
2.564	1.155	$0 \to 2$	100		
2.948	0.408	$6 \to 4$	100		
2.959	1.550	$2 \to 2$	43±3	37±5	49±5
	2.959	$2 \to 0$	57±3	63±5	51±5
3.164	1.755	$2 \to 2$	24±3	17±4	23±4
	3.164	$2 \to 0$	76±3	83±4	77±4
3.296	0.756	$3,4 \to 4$	79±3		
	1.887	$3,4 \to 2$	21±3		
3.345	0.805	$3 \to 4$	39±3	43±10	
	1.936	$3 \to 2$	61±3	57±10	
3.838	0.548	$4 \to 3,4$	≦2	7	
	1.298	$4 \to 4$	9±3	5	
	2.429	$4 \to 2$	91±3	88±5	
4.029	0.733	$J \to 3,4$	95±3		
	1.498	$J \to 4$	5±3		
4.048	0.703	$(4) \to 3$	50±3		
	1.508	$(4) \to 4$	≦2		
	2.639	$(4) \to 2$	50±3		
4.074	1.534	$3 \to 4$	8±3		
	2.665	$3 \to 2$	92±3		
4.265	1.725	$(4) \to 4$	79±14		
	2.856	$(4) \to 2$	21±6		
4.287	2.878	$(0) \to 2$	100		
4.579	3.170	$2 \to 2$	70±10		
	4.579	$2 \to 0$	30±10		
4.656	1.360	$J \to 3,4$	100		
4.700	1.355	$J \to 3$	≧90		
	2.160	$J \to 4$	≦10		
4.781	1.436	$3 \to 3$	11±3		
	1.485	$3 \to 4,3$	18±4		
	2.241	$3 \to 4$	17±4		
	3.372	$3 \to 2$	54±7		
4.949	2.001	$4 \to 6$	10±3		
	2.409	$4 \to 4$	55±5		
	3.540	$4 \to 2$	35±8		

[a]) Ref. [7]). [b]) Ref. [34]).

TABLE 3
Multipole mixing ratios for transitions in ^{54}Fe

Level	E_γ (MeV)	$J_i \to J_f$	E2/M1	Other values
2.959	1.550	$2 \to 2$	$0.105 \pm^{0.040}_{0.042}$	0.25 ± 0.19 [a]), $0 \leqq \delta \leqq 2.2$ [b])
3.164	1.755	$2 \to 2$	$0.63 \pm^{0.57}_{0.25}$, $\delta \geqq 2.4$ $\delta \leqq -10$	$-0.60 \pm^{0.40}_{0.34}$, $\lvert\delta\rvert \geqq 3$ [a])
3.296	0.756	$4 \to 4$	$-1.1 \leqq \delta \leqq -0.67$, $-0.24 \leqq \delta \leqq 0.18$	
	0.756	$3 \to 4$	$0.38 \leqq \delta \leqq 1.66$	
	1.887	$3 \to 2$	$-12 \leqq \delta \leqq -0.25$	
3.345	0.806	$3 \to 4$	0 ± 0.14, $\delta \geqq 3.5$	
	1.936	$3 \to 2$	$-0.65 \pm^{0.18}_{2.25}$	
4.029	0.733	$5 \to 4$	0.27 ± 0.07	
	0.733	$3 \to 4$	$-1.2 \pm^{0.82}_{1.5}$	
	0.733	$4 \to 3$	0.27 ± 0.09	
	0.733	$2 \to 3$	$-9 \leqq \delta \leqq -0.43$	
4.048	0.703	$2 \to 3$	$-2.75 \leqq \delta \leqq -0.38$	
	0.703	$4 \to 3$	0.23 ± 0.09	
4.074	2.665	$3 \to 2$	$1.88 \pm^{0.50}_{0.44}$	
4.265	1.725	$3 \to 4$	$0.91 \pm^{0.73}_{0.39}$	
	1.725	$4 \to 4$	-0.53 ± 0.24	
4.287	2.879	$1 \to 2$	All values of δ	
	2.879	$2 \to 2$	$0.40 \pm^{0.07}_{0.04}$, $\delta \leqq -14$	
	2.879	$3 \to 2$	$-0.16 \pm^{0.05}_{0.01}$	
4.579	3.170	$2 \to 2$	-0.105 ± 0.09, -1.8 ± 0.5	
4.781 [a])	3.372	$3 \to 2$	-0.018 ± 0.026	
4.949	2.409	$4 \to 4$	$-0.36 \pm^{0.2}_{0.3}$	

[a]) Ref. [7]). [b]) Ref. [34]).
[b]) This state is known to have negative parity thus the mixing ratio is δ(M2/E1).

however, between the multipole mixing ratio for the $2_3^+ \to 2_1^+$ transition determined here and that from the work of Thomas *et al.* [7]). This discrepancy is not understood at the present time.

The Doppler-shift analysis is summarized in table 4. In most cases, only the gamma transition which gave the most precise value of $\Delta E/\Delta E_0$ is given, in cases where two transitions were analyzed for a given state, the lifetime derived was based on the weighted average of the two values of $\Delta E/\Delta E_0$. For gamma rays having values of $\Delta E/\Delta E_0$ less than 0.11 †, the present analysis indicates only that the lifetime is longer

† This is the apparent Doppler shift due to recoils which escape the target.

TABLE 4

Mean lifetimes for states in ^{54}Fe from the Doppler-shift attenuation analysis

Level	E_γ (MeV)	E_0 (keV)	E (keV)	$\Delta E/\Delta E_0$	τ (psec)
1.409	1.409	6.56	1.31±0.2	0.200±0.03	$1.1\pm^{0.50}_{0.32}$
2.540	1.131	5.03	0.3 ±0.2	0.06 ±0.04	≧ 3
2.564	1.155	5.13	0.6 ±0.3	0.12 ±0.04	≧ 2
2.948	0.408	1.82	0 ±0.4	≦ 0.22	≧ 0.8
2.959	1.550	6.89	4.82±0.30	0.700±0.04	0.075±0.012
	2.959	13.14	8.77±0.38	0.677±0.03	
3.164	3.164	13.95	5.63±0.5	0.404±0.036	$0.23\pm^{0.05}_{0.04}$
3.296	1.887	8.31	0.4 ±0.5	≦ 0.11	≧ 3
3.345	1.936	8.53	0.5 ±0.6	≦ 0.13	≧ 3
3.838	2.429	10.46	6.57±0.5	0.628±0.045	0.091±0.02
4.029	0.733	3.12	0 ±0.6	≦ 0.16	≧ 1
4.048	2.639	11.26	3.08±1.0	0.274±0.09	$0.44\ \pm^{0.34}_{0.15}$
4.074	2.665	11.36	7.29±0.76	0.642±0.07	0.084±0.025
4.265	1.725	7.30	4.05±0.5	0.550±0.07	$0.119\pm^{0.033}_{0.025}$
4.287	2.878	12.18	7.98±0.7	0.655±0.06	$0.080\pm^{0.024}_{0.020}$
4.579	3.170	13.27	13.33±0.7	1.00±0.05	≦ 0.01
4.656	1.360				
4.700	1.355	unresolved			
4.781	3.372	13.99	10.73±0.76	0.767±0.054	0.048±0.016
	3.372(DE)	13.99	11.34±0.9	0.811±0.065	
4.949	2.409	9.93	7.98±0.6	0.804±0.075	0.042±0.015

than (or equal to) a certain limit. This limit is set by the value $\Delta E/\Delta E_0$+error $(\Delta E/\Delta E_0)$.

The data from tables 2, 3 and 4 have been combined to produce the reduced transition probabilities given in table 5. For transitions where more than one δ was possible, we have included only the solution considered to be most likely. Furthermore, the parity of all states except the 4.781 MeV 3^- was assumed to be positive. Thus, for the former states, E2 and M1 transition probabilities are given. The errors in the derived quantities (e.g., BE2 or BM1) were obtained combining the errors in the branching ratios, mixing ratios, and lifetimes in quadrature, this was done separately for the upper and for the lower limits of the BE2 or BM1.

5. Discussion

In order to discuss the implications of the measured electromagnetic transition data, it is essential to have some idea of what kinds of states to expect in the low-energy

TABLE 5

Electromagnetic transition probabilities for ^{54}Fe derived from tables 2–4

Level	E_γ (MeV)	$J_i^\pi \to J_f^\pi$	δ(E2/M1)	BE2($e^2 \cdot fm^4$)	BE2 (W.u.)	(M1) (eV)	BM1 (W.u.)
1.409	1.409	$2^+ \to 0^+$	0	$133 \pm^{55}_{41}$			
				102 ± 4 [a])	8.4 ± 0.3		
2.540	1.131	$4^+ \to 2^+$	0	$\leqq 147$	$\leqq 12$		
2.564	1.155	$0^+ \to 2^+$	0	$\leqq 199$	$\leqq 16$		
2.959	1.550	$2^+ \to 2^+$	$0.105 \pm^{0.040}_{0.042}$	$5.7 \pm^{5.1}_{3.7}$	$0.47 \pm^{0.42}_{0.30}$	3.73×10^{-3}	0.048 ± 0.008
	2.959	$2^+ \to 0^+$	0	27.2 ± 4.5	2.25 ± 0.4		
				45 ± 5 [b])			
3.164	1.755	$2^+ \to 2^+$	$0.63 \pm^{0.57}_{0.25}$	$12.7 \pm^{20}_{7.8}$	$1.0 \pm^{1.7}_{0.6}$	4.3×10^{-4}	$0.0038 \pm^{0.0013}_{0.002}$
	3.164	$2^+ \to 0^+$	0	8.8 ± 1.9	0.73 ± 0.16		
3.296	1.887	$(4^+) \to 2^+$	0	$\leqq 2.4$	$\leqq 0.2$		
3.345	1.936	$3^{(+)} \to 2^+$	$-0.65 \pm^{0.18}_{2.25}$	$\leqq 5.4$	$\leqq 0.45$	$\leqq 1.1 \times 10^{-4}$	$\leqq 0.0007$
3.838	1.298	$4^+ \to 4^+$	0			6.5×10^{-4}	0.014 ± 0.006
	2.429	$4^+ \to 2^+$	0	96.1 ± 21	8.0 ± 1.8		
4.048	0.703	$(4^+) \to 3^{(+)}$	0.23 ± 0.09	$270 \pm^{270}_{203}$	$22 \pm^{22}_{16}$		
	0.703	$(2^+) \to 3^{(+)}$	$-1.2 \pm^{0.82}_{1.5}$	$3180 \pm^{2270}_{2860}$	$263 \pm^{187}_{237}$		

	2.639	$(4^+) \to 2^+$	0	$7.2 \pm^{3.8}_{3.1}$	$0.6 \pm^{0.30}_{0.26}$		
4.074	1.534	$3^{(+)} \to 4^+$	0			6.3×10^{-4}	0.0083 ± 0.004
	2.665	$3^{(+)} \to 2^+$	$1.88 \pm^{0.50}_{0.44}$	51.7 ± 16	4.3 ± 1.3	1.6×10^{-3}	0.004 ± 0.002
4.265	1.725	$(4^+) \to 4^+$	-0.53 ± 0.24	77.6 ± 55	6.4 ± 4.5	3.4×10^{-3}	0.032 ± 0.011
	2.856	$(4^+) \to 2^+$	0	7.6 ± 2.9	0.63 ± 0.24		
4.287	2.879	$(0^+) \to 2^+$	0	51.5 ± 14	4.3 ± 1.2		
4.579	3.170	$2^{(+)} \to 2^+$	-0.105 ± 0.09	$\geqq 0.04$	$\geqq 0.003$	$\geqq 3.8 \times 10^{-2}$	$\geqq 0.057$
	4.579	$2^{(+)} \to 0^+$	0	$\geqq 12$	$\geqq 1$		
4.949	2.001	$4^{(+)} \to 6^+$	0	60.3 ± 28	5.0 ± 2.3		
	2.409	$4^{(+)} \to 4^+$	$-0.36 \pm^{0.2}_{0.3}$	$15 \pm^{24}_{12}$	$1.2 \pm^{2.0}_{0.9}$	7.6×10^{-3}	0.026 ± 0.01

Level	E_γ (MeV)	$J_i^\pi \to J_f^\pi$		δ(M2/E1)	BE1($e^2 \cdot fm^2$)	BE1 (W.u.)
4.781	1.436	$3^- \to 3^+$	0	0	4.9×10^{-4}	$(5.3 \pm 2.3) \times 10^{-4}$
	1.485	$3^- \to 4^+, 3^+$		0	7.2×10^{-4}	$(7.8 \pm 3.1) \times 10^{-4}$
	2.241	$3^- \to 4^+$		0	2.0×10^{-4}	$(2.1 \pm 0.9) \times 10^{-4}$
	3.372	$3^- \to 2^+$		0	1.84×10^{-4}	$(1.90 \pm 0.7) \times 10^{-4}$

[a]) From ref. [29]).

spectrum of ^{54}Fe. For this purpose, we have used a model proposed by Bansal and French [35]) to estimate the positions of particle-hole (p-h) states on the basis of empirical data. Approximating the p-h interaction by a monopole potential $V_{ph} = -a + b\tau_1 \cdot \tau_2$ we get the following expression for the center of gravity of the np–mh multiplets in ^{54}Fe:

$$E(n\text{p}\text{–}m\text{h}) = M(n\text{p}, t_p) + M(m\text{h}, t_h) - M(^{56}\text{Ni}) - M(^{54}\text{Fe}) - nma + \tfrac{1}{2}b[t(t+1) - t_p(t_p+1) - t_h(t_h+1)] + c, \quad (12)$$

where $M(n\text{p}, t_p)$ is the mass of the state with n particles outside the ^{56}Ni core coupled to isospin t_p; the other terms are defined analogously. The Coulomb energy, c, between proton particles and holes can be estimated by comparing series of isospin multiplets [i.e. ^{58}Ni(g.s.)+^{52}Fe($T = 1$) to ^{58}Cu($T = 1$), ^{52}Mn($T = 1$)]. We obtain consistently $c = -0.25$ MeV. The parameter b describing the isospin splitting was found to be 2.1 ± 0.2 MeV by Sherr *et al.* [36]). The parameter a is less well determined. Depending on the states used in eq. (12), one finds values from -0.04 to -0.25 MeV. We have chosen to use $a = -0.12$. The p–h spectrum of ^{54}Fe using these parameters is given in table 6.

TABLE 6
Estimations of the centers of gravity of particle-hole multiplets

Configuration	t_p	t_h	t	E (MeV)
2p-4h	1	0	1	2.57±1.0
1p-3h	$\frac{1}{2}$	$\frac{1}{2}$	1	4.04±0.43
2p-4h	1	2	1	4.81±1.60
1p-3h	$\frac{1}{2}$	$\frac{3}{2}$	1	5.13±0.63
4p-6h	0	1	1	6.40±3.00
2p-4h	1	1	1	6.66±1.2
1p-3h	$\frac{1}{2}$	$\frac{3}{2}$	2	9.33±1.03
4p-6h	1	1	1	9.36±3.2
4p-6h	1	2	1	13.6 ±3.6
4p-6h	2	2	1	12.1 ±4.00

It is apparent, on the basis of these calculations, that one should not be surprised at the complexity of the low-energy spectrum of ^{54}Fe. In particular, states of the configuration 2p–4h should be found at quite low excitation energy. In addition, within errors, one might possibly find even more complex structures (i.e. 4p–6h states) at rather low energy. In the light of the present estimates and drawing on evidence from two theoretical calculations, we shall see whether the low-lying states of ^{54}Fe can be qualitatively understood.

It is clear if one compares the spectra of ^{54}Fe and ^{50}Ti, that the $2^+, 4^+, 6^+$ sequence in ^{54}Fe must be in large part $(f_{\frac{7}{2}})_J^{-2}$. The first "intruder" state, the 0_2^+ at 2.540 MeV, is a good candidate for the configuration [2p($T = 1$)–4h($T = 0$)] predicted to lie at

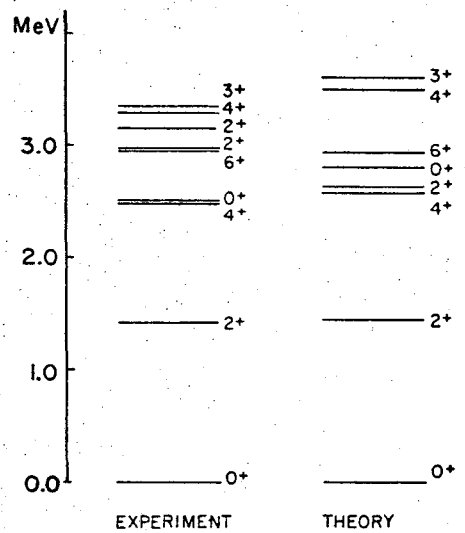

Fig. 18. Comparison of theory to experiment for the low-lying levels of ^{54}Fe. The theoretical calculations are by Lips and McEllistrem [38]).

2.57 MeV. A calculation by Pittel [37]) of the 0^+ states of ^{54}Fe using the Kuo and Brown renormalized matrix elements gives a 0^+ state of the above configuration at 2.52 MeV. Strong evidence for assigning this structure to the 2.54 MeV state comes from the fact that it is strongly excited in the ^{56}Fe(p, t)^{54}Fe reaction. Our data give only an upper limit for the lifetime of the 0_2^+ state.

States in the region of 3–4 MeV may be of the type 1p-3h or 2p-4h. Lips and McEllistrem [38]) (LM) have considered the former in a series of calculations of $N = 28$ nuclei. In the simplest version of their model, proton excitations of the type $(f_{\frac{7}{2}}^{-3}, 2p_{\frac{3}{2}})_J$ were considered. The energy levels they obtained are shown in fig. 18. Expanding the configuration space to the $1f_{\frac{5}{2}}$ shell did little to the positions of the levels. In view of our goal of understanding the gross features of the spectrum of ^{54}Fe we shall only summarize the successes and failures of the proton-excitation model. First on the basis of the evidence given in table 7 it is quite plausible that the 3^+, and 4^+, states are due to the configuration $(f_{\frac{7}{2}}^{-3}, 2p_{\frac{3}{2}})$, although in view of the energies given in table 6, these states could contain as well, components of neutron p-h excitations. The model under consideration does not predict a third 2^+ state at low excitation energy. Furthermore, the theoretical lifetime of the 2_2^+ state is definitely at odds with the measured value. This, again, may be due to the fact that neutron excitations were neglected; but this is only one possible explanation. Finally, it is interesting that LM predict a low-lying 0^+ state of the type 1p-3h. This seems in contradiction with the (p, t) data and the calculations of Pittel. However, this state might contain extensive admixtures of 1p-3h since such configurations are apparently expected in the low energy spectrum. In attempting to learn more of the structure of

TABLE 7

Comparison of experimental and theoretical half-lives, mixing ratios, and branching ratios for ^{54}Fe

Level or transition	E (MeV)		Calc.	Exp.
2_1^+	1.408	$t_{\frac{1}{2}}$	2.12	$0.76\ ^{+0.35}_{-0.22}$
4_1^+	2.539	$t_{\frac{1}{2}}$	8.14	$\geqq 2.1$
0_2^+	2.564	$t_{\frac{1}{2}}$	16.2	$\geqq 1.4$
6_1^+	2.948	$t_{\frac{1}{2}}$	3565	$\geqq 0.56$
2_2^+	2.961	$t_{\frac{1}{2}}$	1.70	0.052 ± 0.008
4_2^+	3.297	$t_{\frac{1}{2}}$	1.08	$\geqq 2.1$
3_1^+	3.345	$t_{\frac{1}{2}}$	5.42	$\geqq 2.1$
$2_2^+ \rightarrow 2_1^+$	1.550	$\lvert\delta\rvert$	0.58	$0.105\pm^{0.040}_{0.042}$
$4_2^+ \rightarrow 4_1^+$	0.756	$\lvert\delta\rvert$	0.53	0.38 to 1.66
$3_1^+ \rightarrow 2_1^+$	1.936	$\lvert\delta\rvert$	0.92	$0.65\ ^{+2.25}_{-0.18}$
$3_1^+ \rightarrow 4_1^+$	0.805	$\lvert\delta\rvert$	0.19	$0.00 \pm 0.14, \geqq 3.5$

Level or transition	E (MeV)		Calc. (%)	Exp. (%)
$2_2^+ \rightarrow 0_1^+$	2.961	branching ratio	72	57
$2_2^+ \rightarrow 2_1^+$	1.550		28	43
$4_2^+ \rightarrow 2_1^+$	1.887	branching ratio	99	21
$4_2^+ \rightarrow 4_1^+$	0.756		1	79
$3_1^+ \rightarrow 2_1^+$	1.936	branching ratio	38	59
$3_1^+ \rightarrow 4_1^+$	0.805		61	41

The theoretical calculations are by Lips [38]). An effective charge of 1.6 e was used in computing the E2 transition strengths. The half-lives are given in ps.

TABLE 8

Comparison of electromagnetic transition probabilities in ^{42}Ca and ^{54}Fe

Transition	$\sigma\lambda$	^{42}Ca	^{54}Fe
$2_1^+ \rightarrow 0_1^+$	E2	8.6 ± 2.0 [a])	8.4 ± 0.8 [b])
$0_2^+ \rightarrow 2_1^+$	E2	65 ± 4 [a])	$\leqq 16$
$2_2^+ \rightarrow 0_1^+$	E2	1.2 ± 0.3 [a])	2.25 ± 0.4
$2_2^+ \rightarrow 2_1^+$	E2	$14.3\ ^{+35}_{-8.5}$ [a])	$0.47\ ^{+0.42}_{-0.30}$
$2_2^+ \rightarrow 2_1^+$	M1	0.091 ± 0.02 [a])	0.048 ± 0.008
$4_1^+ \rightarrow 2_1^+$	E2	1.0 ± 0.3 [c])	$\leqq 12$

[a]) Ref. [40]). [b]) Ref. [29]). [c]) Ref. [41]).

^{54}Fe, it is useful to compare the nuclei ^{54}Fe and ^{42}Ca. In both cases, one observes additional states complicating a $(f_{\frac{7}{2}})^2$ spectrum. In ^{42}Ca, the extra state and the remarkably enhanced $0_2^+ \rightarrow 2_1^+$ transition have been successfully explained by Gerace and Green [39]) as being due to a low-lying band of deformed 4p-2h states which mix with the 2^+ and 0^+ of the $(f_{\frac{7}{2}})^2$ configuration. The analogy as table 8 shows is not inconsistent with the present data. However, an important piece of evidence, the $0_2^+ \rightarrow 2_1^+$ transition strength, is available only as a lower limit. The 0_2^+ state in ^{54}Fe is at higher energy and therefore one might expect less enhancement of the $0_2^+ \rightarrow 2_1^+$ transition.

With regard to the states above the 3_1^+, although much information is available, one cannot, at the present time, offer even a qualitative evaluation of the configurations involved. Shell-model calculations of immense complexity would be required to serve as a reliable guide. One remarkable feature should nevertheless be pointed out. There appears to be two kinds of states between 3.8 and 5 MeV, those which decay to the $(f_{\frac{7}{2}})^{-2}$ states and those which favor decay to the 3_1^+ and 4_2^+ states. This evidence suggests a more complicated structure for these latter states than was previously indicated.

In summary, the present experiment has yielded considerable information about the electromagnetic decays of the excited states of ^{54}Fe below 5 MeV. In addition, numerous spin assignments have been made on the basis of angular correlation data. Estimates using the model of Bansal and French, show that one should expect 2p-1h states at low excitation energy as well as states of the configuration 1p-3h. The 0_2^+ state would appear to be 2p-4h on the basis of the ^{56}Fe(p, t)^{54}Fe reaction. The proton excitation model of Lips and McEllistrem accounts well for the positions of the 2_2^+, 3_1^+, and 4_2^+ states, however, it fails to account for the presence of the 2_3^+ state and does not correctly predict the lifetime of the 2_2^+ state. Although much electromagnetic transition data is available, further elucidation of the structure of ^{54}Fe, with particular interest toward deformed states in analogy to ^{42}Ca, requires measurement of the lifetimes of the 0_2^+, 3_1^+, and 4_2^+ states. In addition, of great interest, would be the observation of ^{54}Fe as the product nucleus in multi-particle transfer reactions.

References

1) J. D. McCullen, B. F. Bayman and L. Zamick, Phys. Rev. **134** (1964) B515
2) H. O. Funsten, N. R. Roberson and E. Rost, Phys. Rev. **134** (1964) B117
3) T. Stovall and N. M. Hintz, Phys. Rev. **135** (1964) B330
4) W. S. Gray, R. A. Kenefick and J. J. Kraushaar, Nucl. Phys. **67** (1965) 565
5) S. F. Eccles, H. F. Lutz and V. A. Madsen, Phys. Rev. **141** (1966) 1067
6) R. J. Peterson, Ph.D. thesis, University of Washington, 1966, unpublished
7) M. F. Thomas, A. R. Poletti and M. A. Grace, Nucl. Phys. **78** (1966) 561
8) A. E. Litherland and A. J. Ferguson, Can. J. Phys. **39** (1961) 788
9) A. R. Poletti and E. K. Warburton, Phys. Rev. **137B** (1965) 595
10) A. J. Ferguson, Angular correlation methods in gamma-ray spectroscopy (North-Holland, Amsterdam, 1965)
11) E. K. Warburton, D. E. Alburger and D. H. Wilkinson, Phys. Rev. **129** (1963) 2180

12) A. E. Blaugrund, Nucl. Phys. **88** (1966) 501
13) R. E. Pixley and W. Benenson, Nucl. Phys. **A91** (1967) 177
14) P. Paul, J. B. Thomas and S. S. Hanna, Phys. Rev. **147** (1966) 774
15) J. Lindhard, M. Scharff and H. E. Schiøtt, Mat. Fys. Medd. Dan. Vid. Selsk. **33** (1963) no. 14
16) D. L. Hendrie, C. Glashausser, J. M. Moss and J. Thirion, Phys. Rev. **186** (1969) 1188
17) F. S. Goulding, D. A. Landis and R. H. Pehl, Lawrence Radiation Lab. Rep., UCRL-17560, unpublished
18) R. E. Hintz, F. B. Selph, W. S. Flood, B. G. Harvey, F. G. Resmini and E. A. McClatchie, Nucl. Instr. **72** (1969) 61
19) D. J. Church, R. N. Horoshko and G. E. Mitchell, Phys. Rev. **160** (1967) 894
20) G. J. Nijgh, A. H. Wapstra and R. van Lieshout, Nuclear spectroscopy tables (North-Holland, Amsterdam, 1959)
21) L. C. Northcliffe, Ann. Rev. Nucl. Sci. **13** (1963) 67
22) M. A. Eswaren, H. E. Gove, A. E. Litherland and C. Broude, Nucl. Phys. **66** (1965) 401
23) P. G. Steward and R. Wallace, University of California, Lawrence Radiation Lab. Rep. UCRL-17314, unpublished
24) A. Aspinall, G. Brown and S. E. Warren, Nucl. Phys. **46** (1963) 33
25) A. Sperduto and W. W. Buechner, Phys. Rev. **134B** (1964) 142
26) O. Hansen, T. A. Belote and W. E. Dorenbusch, Nucl. Phys. **A118** (1968) 41
27) D. Wegener, Z. Phys. **198** (1967) 251
28) D. H. Wilkinson, Nuclear spectroscopy, part B, ed. F. Ajzenberg-Selove (Academic Press, New York, 1960) p. 852
29) J. J. Simpson, J. A. Cookson, D. Eccleshall and M. J. L. Yates, Nucl. Phys. **62** (1965) 385
30) J. Bellicard and P. Barreau, Nucl. Phys. **36** (1962) 476
31) D. C. Sutton, H. A. Hill and R. Sherr, Bull. Am. Phys. Soc. **4** (1959) 278
32) T. A. Belote, W. E. Dorenbusch and O. Hansen, Nuclear spin-parity assignments., ed. N. B. Gove (Academic Press, New York, 1966) p. 350
33) C. F. Perdrisat, Rev. Mod. Phys. **38** (1966) 41
34) R. W. Benjamin and I. L. Morgan, Phys. Rev. **163** (1967) 1252
35) R. K. Bansal and J. B. French, Phys. Lett. **11** (1964) 145
36) R. Sherr *et al.*, Phys. Rev. **139** (1965) 1272
37) S. Pittel, Phys. Lett. **33B** (1970) 158
38) K. Lips and M. T. McEllistrem, Phys. Rev. **1C** (1970) 1009;
K. Lips, to be published
39) W. J. Gerace and A. M. Green, Nucl. Phys. **A93** (1967) 110
40) W. J. Kossler, J. Winkler and C. D. Kavaloski, Phys. Rev. **177** (1969) 1725
41) R. R. Hartmann, K. P. Lieb and H. Ropke, Nucl. Phys. **A123** (1969) 437

TECHNICAL INFORMATION DIVISION
LAWRENCE BERKELEY LABORATORY
UNIVERSITY OF CALIFORNIA
BERKELEY, CALIFORNIA 94720